

# An Unfitted Interface Penalty DG–FE Method for Elliptic Interface Problems

Juan Han<sup>\*</sup> Haijun Wu<sup>†</sup> and Yuanming Xiao<sup>‡</sup>

## Abstract

We design an unfitted interface penalty DG-FE Method (UIPDG-FEM) for an elliptic interface problem, which uses the interior penalty discontinuous Galerkin methods locally along the interface together with additional penalty terms on the interface (or the Nitsche’s trick) to deal with the jump conditions, and uses the finite element methods away from the interface. Moreover, the trick of merging elements is used to keep the condition number of the algebraic system not affected by the interface position. The proposed UIPDG-FEM not only possesses flexibilities of the IPDG method, in particular, simplifying the process of merging elements near a complex interface, but also avoids its drawback of larger number of global degrees of freedom. The convergence rates of the UIPDG-FEM solution are optimal and independent of the interface position. Furthermore, a uniform estimate of the flux value is established in terms of the discontinuous physical coefficients. A two dimensional merging algorithm is also presented, which is guaranteed to succeed under appropriate assumptions on the interface. Numerical examples are given to verify the theoretical results.

**Key words:** elliptic interface problem, unfitted meshes, interface penalty DGM, FEM, harmonic weighting, flux estimates, merging algorithm.

## 1 Introduction

Interface problems have a wide range of applications in engineering and science, particularly in fluid dynamics and materials science. Examples of interface problems include multiphase flow, crystal growth, modeling of the Stefan problem in solidification processes, composite materials, cell and bubble deformation, and fiber suspension. The partial differential equations that describe these applications typically have discontinuous coefficients across interfaces. Due to the low global regularity of the solution and the irregular geometry of the interface, designing highly efficient numerical methods for these equations is challenging.

Over the past few decades, various numerical approaches have been proposed in the literature for solving second order elliptic interface problems. These methods can generally be classified into two categories: body-fitted and unfitted methods. Body-fitted methods use meshes almost aligned with the interface to resolve the discontinuity, and the classical finite element schemes can be directly applied to such meshes. [14] discusses the linear finite element case, and [30] combines the

---

<sup>\*</sup>Department of Mathematics, Nanjing University, Nanjing 210093, China. Email address: dg20210004@smail.nju.edu.cn

<sup>†</sup>Department of Mathematics, Nanjing University, Nanjing 210093, China. Email address: hjw@nju.edu.cn

<sup>‡</sup>Department of Mathematics, Nanjing University, Nanjing 210093, China. Email address: xym@nju.edu.cn

isoparametric technique to give a high-order form. However, it is challenging and computationally expensive to generate and refine a good body-fitted mesh that follows the highly dynamic movement of the interface in many situations, especially when a moving interface is involved.

To reduce the high cost of mesh generation, there has been a notable surge in interest towards unfitted methods. In these methods, the interface is permitted to cross through elements rather than confining the mesh, and discontinuity can be distributed within the elements. In order to characterize the discontinuity, the finite element space needs to be modified in order to satisfy the interface conditions, approximately or weakly, such as the immersed finite element method [32], or use sliced polynomials on the interface elements. If the second strategy is adopted, two sets of degrees of freedom are required in the interface elements, and it is better to weakly impose the Dirichlet jumps on the interface. Inspired by the Nitsche penalty method [35] and the Lagrange multiplier method [2] for weakly imposing Dirichlet boundary conditions, quite a few numerical methods in this category have been proposed and studied. For example, the multiscale unfitted finite element method [15], the cut finite element method [10], the  $hp$ -interface penalty finite element method [39], the unfitted discontinuous Galerkin methods [4, 33, 37]. Furthermore, considering the uncertainty of the intersection between the interface and the mesh, some element (say  $K$ ) may intersect a certain subregion with a small area, that is,  $|K \cap \Omega_i| \ll |K|$ . Aggregation of such elements may lead to an ill-conditioned discrete algebraic system. For brevity, we refer to them as small elements. There are mainly two strategies to mitigate the impact of small elements on the condition number. One is incorporating “ghost penalties” [5] into the bilinear form, where in addition to the penalty terms on the interface, the penalties are also applied to the jumps of derivatives (with orders up to the degree of the piecewise of polynomials) at the faces of elements crossed by the interface. The other is establishing a dependence for the degrees of freedom between small elements with their surrounding elements, its objective is to modify the finite element space in a way that eliminates small elements, thus addressing the issue of condition number. For example, The patch reconstruction DG method [31] combines the DG method with the least square method. The aggregated unfitted finite element method [3] deals with the degrees of freedom in small elements by extrapolation, which is easy to be implemented but may cause instability issues when high-order finite elements are used. In contrast, the merging element methods [13, 26, 27] merge the small elements with their appropriate neighbor elements so that the merged macro-elements are not small. This idea is also extend to unfitted HHO method with cell agglomeration [6, 8] which allows meshes including polygonal elements. There have been algorithms of merging elements in the literature for non-conforming meshes [13] and unfitted HHO method [6]. The merging algorithm for conforming meshes is slightly delicate since the hanging nodes must be carefully handled, whereas it is somewhat more natural for discontinuous Galerkin methods.

In this paper, we propose an unfitted interface penalty DG–FE Method (UIPDG-FEM) for an elliptic interface problem, which uses the interior penalty discontinuous Galerkin methods locally along the interface together with additional penalty terms on the interface (or the Nitsche’s trick) to dealing with the jump conditions, and use the finite element methods away from the interface. In addition, the trick of merging elements is used to keep the condition number of the algebraic system not affected by the interface position relative to the meshes. The proposed UIPDG-FEM not only possesses flexibilities of the IPDG method, in particular, simplifying the process of merging elements near complex interface, but also avoids its drawback of larger number of global degrees of freedom since the DG scheme is only used locally near the interface. In particular, the UIPDG-FEM does not suffer the problem of instability since the extrapolation is not used here. Moreover, the UIPDG-FEM also exhibits the following desirable characteristics possessed by several other effective

unfitted methods [3,6,26]: The method is of arbitrary high order with optimal convergence rate; The error bound of the flux is also optimal and uniform in terms of the discontinuous coefficients; The condition number of the stiffness matrix is independent of the location of the interface relative to the meshes. Furthermore, we introduce a feasible and reliable merging algorithm for two dimensional interface problems, which allows a wider variety of interface elements than [13] and [6]. In particular, we use two geometric variables related to the interface and the mesh size to define whether the interface is well resolved by the meshes. Under appropriate conditions (see Assumption (I)-(III)), we provide a proof of the feasibility of the algorithm, that is, each small element has a large element that can be merged, and a proof of the reliability of the algorithm, that is, the mesh obtained by merging Algorithm 5.1 has no overlapped elements and its mesh size is equivalent to the one of the original mesh before merging.

The rest of our paper is organized as follows. In Section 2, we present the formulation of the UIPDG-FEM. Well-posedness and error estimates for symmetric UIPDG-FEM are presented in Section 3, including the error estimates of the solution in the energy and  $L^2$  norms and the error estimate of the flux in the  $L^2$  norm. In section 4, we analyze the condition number of the discrete system. In Section 5, we construct a merging algorithm for the two dimensional case and prove its feasibility and reliability. In Section 6, we present some numerical experiments to confirm the theoretical findings.

## 2 The unfitted interface penalty DG–FE Method

Let  $\Omega$  be a convex polygon in  $\mathbb{R}^d$ ,  $d = 2$ , or  $3$ . Suppose  $\Omega$  contains two subdomains  $\Omega_i \subset \Omega$  ( $i = 1, 2$ ) separated by a  $C^2$ -smooth interior interface  $\Gamma = \partial\Omega_1 = \partial\Omega_1 \cap \partial\Omega_2$ . We consider the model problem

$$(2.1) \quad \begin{cases} -\nabla \cdot (\alpha \nabla u) = f & \text{in } \Omega_1 \cup \Omega_2, \\ [u] = g_D, \quad [(\alpha \nabla u) \cdot \mathbf{n}] = g_N & \text{on } \Gamma, \\ u = 0 & \text{on } \partial\Omega. \end{cases}$$

Here  $\alpha = \alpha_i$ ,  $i = 1, 2$ , is a piecewise constant function on the partition  $\Omega_1 \cup \Omega_2$ ,  $\mathbf{n}$  is the unit vector normal to  $\Gamma$ , outward-directed with respect to  $\Omega_1$ , and  $[v] = (v_1 - v_2)|_\Gamma$ , where  $v_i = v|_{\Omega_i}$ ,  $i = 1, 2$ .

Throughout the paper,  $C$  is used to denote a generic positive constant which is independent of the mesh size  $h$ , the coefficient  $\alpha$ , the penalty parameters, and the location of the interface relative to the meshes. We also use the shorthand notation  $A \lesssim B$  and  $B \gtrsim A$  for the inequality  $A \leq CB$  and  $B \geq CA$ .  $A \approx B$  is for the statement  $A \lesssim B$  and  $B \lesssim A$ .

To formulate our UIPDG-FEM, we need to introduce some notions. Let  $\{\mathcal{T}_h\}$  be a family of conforming, quasi-uniform, and regular partitions of the domain  $\Omega$  into parallelograms/parallelepipeds. For any  $K \in \mathcal{T}_h$ , let  $\mathcal{Q}_p(K)$  be the set of all polynomials whose degrees in each variable are less than or equal to  $p$ . Define the continuous  $p$ -th order finite element space on  $\mathcal{T}_h$  by

$$U_h := \{v_h \in H_0^1(\Omega) : v_h|_K \in \mathcal{Q}_p(K), \forall K \in \mathcal{T}_h\}.$$

For any  $K \in \mathcal{T}_h$ , let  $h_K$  be the maximum length of edges of  $K$ . Let  $h := \max_{K \in \mathcal{T}_h} h_K$ . Then  $h_K \approx h$ . Note that any element  $K \in \mathcal{T}_h$  is considered as closed. Let  $\mathcal{T}_\Gamma = \{K \in \mathcal{T}_h : K^\circ \cap \Gamma \neq \emptyset\}$  be the set of all elements that intersect the interface, where  $K^\circ$  denotes the interior of  $K$ . In this paper we assume the finite element mesh is fine enough to resolve the interface, that is,  $0 < h \leq h_0$  for some

$h_0$  depends on the curvature of the interface (see Lemma 3.1 below and also Lemma 3.1 in [39, 40] for a characterization of  $h_0$ ). Set  $\mathcal{T}_{h,i} = \{K \in \mathcal{T}_h : K \cap \Omega_i \neq \emptyset\}$  ( $i = 1, 2$ ). Clearly,  $\mathcal{T}_\Gamma \subset \mathcal{T}_{h,i}$ . Note that an element in  $\mathcal{T}_\Gamma$  may have “small” intersection with  $\Omega_i$  which may cause instability issues in the unfitted methods. Hansbo *et al.* [24] used a suitable weighted flux average along with the Nitsche’s trick to ensure the discrete coercivity but the discrete linear system may be ill-conditioned. Burman [5] proposed further the ghost penalty technique to solve the ill-conditioned issue but did not consider the dependence on jump of the coefficients. Hou *et al.* [15] proposed a multiscale finite element method whose error in energy norm is independent of jump of the coefficient but is only of first order. In this paper, we borrow the ideas of harmonic weighting from Burman and Zunino [11] along with the Nitsche’s trick to construct an arbitrary order unfitted method whose error estimate in energy norm is quasi-optimal, independent of jump of the coefficient and the relative position of the interface to the meshes. Furthermore, we incorporate the concept of merging elements from [26] to ensure that the condition number of the stiffness matrix remains independent of the relative position of the interface to the meshes. Additionally, we introduce the flexibility of allowing the merged element and its adjacent elements to be discontinuous. This approach not only simplifies the implementation process of merging but also provides an easily definable degree of freedom, making it capable of handling slightly more complex interface scenarios.

As previously discussed, the initial step is to merge small elements and define the finite element space. Suppose we have a fixed threshold value  $\delta \in (0, 1/2)$ , We classify an element  $K \in \mathcal{T}_\Gamma$  as having a small intersection with  $\Omega_i$  if the following condition is met:

$$(2.2) \quad |K \cap \Omega_i| < \delta|K|.$$

Conversely, if the above condition is not satisfied, we classify the element as having a large intersection with  $\Omega_i$ . Based on this criterion, we split  $\mathcal{T}_{h,i}$  into two subsets

$$(2.3) \quad \mathcal{T}_{h,i}^{small} = \{K \in \mathcal{T}_\Gamma : |K \cap \Omega_i| < \delta|K|\}, \quad \mathcal{T}_{h,i}^{large} = \mathcal{T}_{h,i} \setminus \mathcal{T}_{h,i}^{small}.$$

When the interface is well resolved, in the two dimensional case, we can construct a merging algorithm (see Algorithm 5.1) to find the macro-element  $M_i(K)$  for each small element  $K \in \mathcal{T}_{h,i}^{small}$ , which must contain an element in  $\mathcal{T}_{h,i}^{large}$ , such that  $|M_i(K) \cap \Omega_i| \approx |M_i(K)|$  and  $h_K \approx h_{M_i(K)}$ . For any two small elements  $K_1$  and  $K_2$  in  $\mathcal{T}_{h,i}^{small}$ ,  $M_i(K_1) = M_i(K_2)$  or  $M_i(K_1)^\circ \cap M_i(K_2)^\circ = \emptyset$  (see Figure 2.1 for an illustration). For other elements in  $\mathcal{T}_{h,i}^{large}$  that are not involved in the merging process, we define  $M_i(K)$  as  $K$  itself. Then the induced mesh of  $\mathcal{T}_{h,i}$  is defined as:  $\mathcal{M}_{h,i} = \{M_i(K) : K \in \mathcal{T}_{h,i}\}$ ,  $i = 1, 2$ .

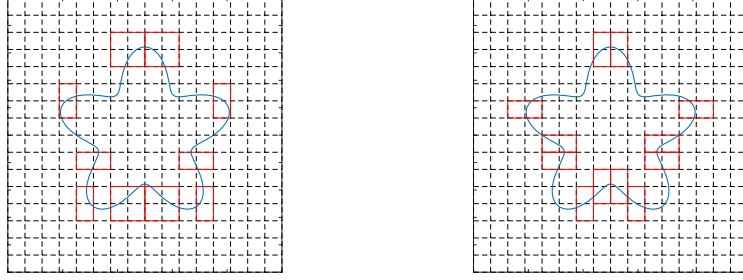
To introduce the variational formulation, let  $\widehat{\Omega}_{h,i} = \bigcup_{K \in (\mathcal{M}_{h,i} \cap \mathcal{T}_{h,i})} K$  be the union of elements not involved in merging, and  $\Omega_{h,i} = \bigcup_{K \in \mathcal{M}_{h,i}} K$ , we define the DG-FE space,

$$V := \left\{ v : v|_{K \cap \Omega_i} \in H^2(K \cap \Omega_i), \forall K \in \mathcal{M}_{h,i} \setminus \mathcal{T}_{h,i}; v|_{\widehat{\Omega}_{h,i} \cap \Omega_i} \in H^1(\widehat{\Omega}_{h,i} \cap \Omega_i), i = 1, 2, v|_{\partial\Omega} = 0 \right\}.$$

and the space of partially discontinuous piecewise polynomials in merged elements as

$$W_{h,i} := \left\{ v_h \in L^2 \left( \bigcup_{K \in \mathcal{M}_{h,i} \setminus \mathcal{T}_{h,i}} K \right) : v_h|_K \in \mathcal{Q}_p(K) \right\}, \quad i = 1, 2.$$

Denote  $U_{h,i} = U_h \cdot \chi_{\widehat{\Omega}_{h,i}}$  the finite element space that is continuous in  $\widehat{\Omega}_{h,i}$ , for  $i = 1, 2$ . Then we define our finite element space  $V_{h,i}$  as the direct sum of  $W_{h,i}$  and  $U_{h,i}$ . That is,  $V_{h,i} := W_{h,i} \oplus U_{h,i}$ ,

(A)  $\mathcal{M}_{h,1}$ (B)  $\mathcal{M}_{h,2}$ Fig. 2.1: Merged elements for  $h = 1/16$ .

for  $i = 1, 2$  and  $V_h$  is

$$V_h := \{v_h = v_{h,1} \cdot \chi_{\Omega_1} + v_{h,2} \cdot \chi_{\Omega_2}, v_{h,i} \in V_{h,i}, i = 1, 2\}.$$

Clearly,  $V_h \subset V$ . In addition, let  $\mathcal{E}_h^i = \{e : e \subset \partial K, e \cap \Omega_i \neq \emptyset, \forall K \in \mathcal{M}_{h,i} \setminus \mathcal{T}_{h,i}\}$ , and  $\mathring{\mathcal{E}}_h^i = \{e \cap \Omega_i : e \in \mathcal{E}_h^i\}$  be the sets of edges that we need.

We will use the notation  $(\cdot, \cdot)_\omega$  for the  $L^2(\omega)$  inner product on  $\omega$  (and similarly for inner products in  $[L^2(\omega)]^d$ ). Let  $H^s(\omega)$  be the Sobolev space with the corresponding usual norm and seminorm, denoted respectively by  $\|\cdot\|_{s,\omega}$  and  $|\cdot|_{s,\omega}$ . Let  $H^s(\Omega_1 \cup \Omega_2)$  be the piecewise  $H^s$  space endowed with norm and seminorm:

$$\|\cdot\|_{s,\Omega_1 \cup \Omega_2} = (\|\cdot\|_{s,\Omega_1}^2 + \|\cdot\|_{s,\Omega_2}^2)^{\frac{1}{2}}, \quad |\cdot|_{s,\Omega_1 \cup \Omega_2} = (|\cdot|_{s,\Omega_1}^2 + |\cdot|_{s,\Omega_2}^2)^{\frac{1}{2}}.$$

For any pair of nonnegative numbers  $w = (w_1, w_2)$  with  $w_1 + w_2 = 1$  and any function  $v \in V$ , we define the following weighted averages of  $v$  on the interface:

$$\{v\}_w := w_1 v_1 + w_2 v_2, \quad \{v\}^w := w_2 v_1 + w_1 v_2,$$

where  $v_i = v|_{\Omega_i}, i = 1, 2$ . When  $w_1 = w_2 = \frac{1}{2}$ , we omit the superscript and subscript. In this paper, we use the following so-called ‘‘harmonic weights’’ as adopted in the discontinuous Galerkin methods [12, 20] on the interface:

$$(2.4) \quad w_1 = \frac{\alpha_2}{\alpha_1 + \alpha_2}, \quad w_2 = \frac{\alpha_1}{\alpha_1 + \alpha_2}.$$

Clearly,  $\{\alpha\}_w = \frac{2\alpha_1\alpha_2}{\alpha_1 + \alpha_2}$  is the harmonic average of  $\alpha_1$  and  $\alpha_2$ , and

$$(2.5) \quad \alpha_{min} \leq \{\alpha\}_w \leq \alpha_{max}, \quad \{\alpha\}^w \leq 2\alpha_{min},$$

where  $\alpha_{min} = \min\{\alpha_1, \alpha_2\}, \alpha_{max} = \max\{\alpha_1, \alpha_2\}$ .

Testing the equation (2.1)<sub>a</sub> by any  $v \in V$ , using integration by parts, and using the ‘‘magic’’ formula  $[ab] = \{a\}_w [b] + [a] \{b\}^w$ , we obtain

$$\int_{\Omega_1 \cup \Omega_2} \alpha \nabla u \cdot \nabla v - \int_{\Gamma} \{(\alpha \nabla u) \cdot \mathbf{n}\}_w [v] - \sum_{i=1}^2 \int_{\mathring{\mathcal{E}}_h^i} \{\alpha_i \nabla u \cdot \mathbf{n}\} [v] = \int_{\Omega_1 \cup \Omega_2} f v + \int_{\Gamma} g_N \{v\}^w.$$

Then define the bilinear form

$$(2.6) \quad \begin{aligned} a_h(u, v) &= \int_{\Omega_1 \cup \Omega_2} \alpha \nabla u \cdot \nabla v - \int_{\Gamma} (\{\alpha \nabla u \cdot \mathbf{n}\}_w [v] + \beta [u] \{\alpha \nabla v \cdot \mathbf{n}\}_w) \\ &\quad - \sum_{i=1}^2 \int_{\mathcal{E}_h^i} \alpha_i (\{\nabla u \cdot \mathbf{n}\}[v] + \beta [u] \{\nabla v \cdot \mathbf{n}\}) + J_0(u, v), \end{aligned}$$

$$(2.7) \quad J_0(u, v) = \int_{\Gamma} \frac{\gamma \alpha_w}{h} [u][v] + \sum_{i=1}^2 \int_{\mathcal{E}_h^i} \frac{\gamma \alpha_i}{h} [u][v].$$

and the linear form

$$(2.8) \quad f_h(v) = \int_{\Omega_1 \cup \Omega_2} f v + \int_{\Gamma} g_N \{v\}^w - \beta \int_{\Gamma} g_D \{\alpha \nabla v \cdot \mathbf{n}\}_w + \int_{\Gamma} \frac{\gamma \{a\}_w}{h} g_D [v],$$

where  $\beta$  is a real number,  $\gamma$  is a positive number to be specified later.

It is easy to check that the solution  $u$  to the problem (2.1) satisfies the following equation:

$$(2.9) \quad a_h(u, v) = f_h(v), \quad \forall v \in V.$$

Inspired by the formulation (2.9), we propose the following unfitted interface penalty DG–FE method: Find  $u_h \in V_h$  such that

$$(2.10) \quad a_h(u_h, v_h) = f_h(v_h), \quad \forall v_h \in V_h.$$

**Remark 2.1.** (i) *The above tricks on dealing with the discontinuities are from the interior penalty discontinuous or continuous Galerkin methods (see, e.g., [7, 21]). When  $\beta = 1$ ,  $a_h(\cdot, \cdot)$  is symmetric, that is, the method is termed as the symmetric unfitted interface penalty DG-FEM (SUIPDG-FEM), which corresponds to the symmetric interior penalty Galerkin method. On the other hand, when  $\beta \neq 1$ ,  $a_h(\cdot, \cdot)$  is non-symmetric. In this paper, for the ease of presentation, we only consider the case  $\beta = 1$ , nevertheless the ideas of this paper also analogously apply to the case  $\beta \neq 1$ .*

(ii) *There are many possible choices of weights other than the harmonic one, i.e., (2.4). As a matter of fact, the estimates in this paper still hold if the weights are so chosen that the weighted average of the coefficient satisfies  $\{\alpha\}_w \lesssim \alpha_{\min}$ . For example, besides (2.4), one can choose  $w_1 = 1, w_2 = 0$  if  $\alpha_1 \leq \alpha_2$  and  $w_1 = 0, w_2 = 1$  if  $\alpha_1 > \alpha_2$ .*

From the equations (2.9) and (2.10), we have the Galerkin orthogonality.

$$(2.11) \quad a_h(u - u_h, v_h) = 0, \quad \forall v_h \in V_h.$$

Next, we introduce the following broken  $H^1$ -norm on the space  $V$ :

$$(2.12) \quad \|v\|_h^2 = \|\alpha^{\frac{1}{2}} \nabla v\|_{0, \Omega_1 \cup \Omega_2}^2 + J_0(v, v) + \frac{h}{\gamma \{\alpha\}_w} \|\{\alpha \nabla v \cdot \mathbf{n}\}_w\|_{0, \Gamma}^2 + \sum_{i=1}^2 \frac{h}{\gamma \alpha_i} \|\{\alpha_i \nabla v \cdot \mathbf{n}\}\|_{0, \mathcal{E}_h^i}^2.$$

### 3 Error estimates of SUIPDG-FEM

In this section, we consider the case of  $\beta = 1$ . We recall some useful results and prove the approximation properties of the discrete spaces.

The following trace and inverse trace inequalities on the elements crossed by the interface are important in the analysis of our method. We refer to [39, Lemma 3.1] for the details of the proof.

**Lemma 3.1.** *There exists a positive constant  $h_0$  depending only on the interface  $\Gamma$  and the shape regularity of the meshes, such that for all  $h \in (0, h_0)$ ,  $K \in \mathcal{M}_{h,i}$ ,  $i = 1$  or  $2$ , the following estimates hold.*

$$(3.1) \quad \|v\|_{0,\Gamma \cap K} \lesssim h_K^{-\frac{1}{2}} \|v\|_{0,K \cap \Omega_i} + \|v\|_{0,K \cap \Omega_i}^{\frac{1}{2}} \|\nabla v\|_{0,K \cap \Omega_i}^{\frac{1}{2}}, \forall v \in H^1(K),$$

$$(3.2) \quad \|v_h\|_{0,\Gamma \cap K} \leq C_{tr1} h_K^{-\frac{1}{2}} \|v_h\|_{0,K \cap \Omega_i}, \forall v_h \in \mathcal{Q}_p(K),$$

and classical trace and inverse trace inequalities, for all  $K \in \mathcal{M}_{h,i}$ ,

$$(3.3) \quad \|v\|_{0,\partial K} \lesssim h_K^{-\frac{1}{2}} \|v\|_{0,K} + \|v\|_{0,K}^{\frac{1}{2}} \|\nabla v\|_{0,K}^{\frac{1}{2}}, \forall v \in H^1(K),$$

$$(3.4) \quad \|v_h\|_{0,\partial K} \leq C_{tr2} h_K^{-\frac{1}{2}} \|v_h\|_{0,K}, \forall v_h \in \mathcal{Q}_p(K).$$

The following lemma is from the standard Sobolev extension property:

**Lemma 3.2.** *Let  $s \geq 1$ . There exist two extension operators  $E_1 : H^s(\Omega_1) \mapsto H^s(\Omega) \cap H_0^1(\Omega)$  and  $E_2 : H^s(\Omega_2) \mapsto H^s(\Omega) \cap H_0^1(\Omega)$  such that*

$$(E_i v)|_{\Omega_i} = v \quad \text{and} \quad \|E_i v\|_{s,\Omega} \lesssim \|v\|_{s,\Omega_i}, \quad \forall v \in H^s(\Omega_i) \quad i = 1, 2.$$

The following lemma which is equivalent to the Bramble-Hilbert Lemma is used in the convergence analysis of the traditional FEM [19].

**Lemma 3.3** (Deny-Lions). *Let  $\Omega$  be a bounded Lipschitz domain. Then there exists a constant  $C(\Omega)$  such that*

$$(3.5) \quad \inf_{q \in \mathcal{Q}_p(\Omega)} \|v + q\|_{p+1,\Omega} \leq C(\Omega) |v|_{p+1,\Omega}, \quad \forall v \in H^{p+1}(\Omega).$$

Next we consider the interpolation error. For any piecewise  $H^2$  function  $v \in H^2(\Omega_1 \cup \Omega_2)$ , let  $v_i = E_i(v|_{\Omega_i})|_{\Omega_{h,i}}$  be the extension of the restriction of  $v$  on  $\Omega_i$  to  $\Omega_{h,i}$ ,  $i = 1, 2$ . Let  $v_{iI} \in V_{h,i}$  be the finite element interpolant of  $v_i$ . Then the interpolant  $I_h v$  of  $v$  onto  $V_h$  is defined by

$$(I_h v)|_{\Omega_i} = v_{iI}|_{\Omega_i}, \quad i = 1, 2.$$

**Lemma 3.4.** *Suppose  $0 < h \leq h_0$ . Then*

$$\|v - I_h v\|_h \lesssim (1 + \gamma + \gamma^{-1})^{\frac{1}{2}} h^p \|\alpha^{\frac{1}{2}} v\|_{p+1,\Omega_1 \cup \Omega_2}, \quad \forall v \in H^{p+1}(\Omega_1 \cup \Omega_2).$$

*Proof.* Denote by  $\eta_i = v_i - v_{iI}$  and by  $\eta = v - I_h v$ . Obviously,  $\eta|_{\Omega_i} = \eta_i|_{\Omega_i}$ ,  $i = 1, 2$ . From the standard finite element interpolation theory [16, 19] we have, for  $i = 1, 2, j = 0, 1, \dots, p+1$ ,

$$(3.6) \quad \left( \sum_{K \in \mathcal{M}_{h,i}} \|v_i - v_{iI}\|_{j,K}^2 \right)^{\frac{1}{2}} \lesssim h^{p+1-j} |v_i|_{p+1,\Omega_{h,i}}.$$

Next we estimate each term in  $\|v_h\|_h$ . Clearly,

$$(3.7) \quad \|\alpha^{\frac{1}{2}} \nabla \eta\|_{0, \Omega_1 \cup \Omega_2}^2 = \sum_{i=1}^2 \|\alpha_i^{\frac{1}{2}} \nabla \eta_i\|_{0, \Omega_i}^2 \lesssim h^{2p} \|\alpha^{\frac{1}{2}} v\|_{p+1, \Omega_1 \cup \Omega_2}^2,$$

From (3.1), (3.6) and  $\{\alpha\}_w \leq 2\alpha_i$ ,  $i = 1, 2$ , denote  $\mathcal{M}_{h,i}^\Gamma$  the set of all elements in  $\mathcal{M}_{h,i}$  that intersect the interface, then

$$(3.8) \quad \begin{aligned} \frac{\gamma\{\alpha\}_w}{h} \|[\eta]\|_{0, \Gamma}^2 &\lesssim \frac{\gamma\{\alpha\}_w}{h} \sum_{i=1}^2 \sum_{K \in \mathcal{M}_{h,i}^\Gamma} \|\eta_i\|_{0, \Gamma \cap K}^2 \\ &\lesssim \frac{\gamma\{\alpha\}_w}{h} \sum_{i=1}^2 \sum_{K \in \mathcal{M}_{h,i}^\Gamma} (h_K^{-1} \|\eta_i\|_{0, K}^2 + \|\eta_i\|_{0, K} \|\nabla \eta_i\|_{0, K}) \\ &\lesssim \frac{\gamma\{\alpha\}_w}{h} \sum_{i=1}^2 \sum_{K \in \mathcal{M}_{h,i}^\Gamma} (h_K^{-1} \|\eta_i\|_{0, K \cap \Omega_i}^2 + \|\eta_i\|_{0, K \cap \Omega_i} \|\nabla \eta_i\|_{0, K \cap \Omega_i}) \\ &\lesssim \frac{\gamma\{\alpha\}_w}{h} \sum_{i=1}^2 h^{2p+1} \|v\|_{p+1, \Omega_i}^2 \\ &\lesssim \gamma h^{2p} \|\alpha^{\frac{1}{2}} v\|_{p+1, \Omega_1 \cup \Omega_2}^2, \end{aligned}$$

From (3.1) and (3.6) again,

$$(3.9) \quad \begin{aligned} \frac{h}{\gamma\{\alpha\}_w} \|\{\alpha \nabla \eta \cdot \mathbf{n}\}_w\|_{0, \Gamma}^2 &\lesssim \frac{h}{\gamma\{\alpha\}_w} \sum_{i=1}^2 \sum_{K \in \mathcal{M}_{h,i}^\Gamma} \|\alpha_i w_i \nabla \eta_i\|_{0, K \cap \Gamma}^2 \\ &\lesssim \frac{h}{\gamma\{\alpha\}_w} \sum_{i=1}^2 \sum_{K \in \mathcal{M}_{h,i}^\Gamma} \alpha_i^2 w_i^2 (h_K^{-1} |\eta_i|_{1, K}^2 + |\eta_i|_{1, K} |\eta_i|_{2, K}) \\ &\lesssim \frac{h}{\gamma} \sum_{i=1}^2 \frac{\alpha_i^2 w_i^2}{\{\alpha\}_w} h^{2p-1} \|v\|_{p+1, \Omega_i}^2 \\ &\lesssim \frac{1}{\gamma} h^{2p} \|\alpha^{\frac{1}{2}} v\|_{p+1, \Omega_1 \cup \Omega_2}^2, \end{aligned}$$

where we have used the following estimate to derive the last inequality:

$$(3.10) \quad \frac{\alpha_i^2 w_i^2}{\{\alpha\}_w} = \frac{\alpha_i w_i}{\{\alpha\}_w} \alpha_i w_i < \frac{1}{2} \alpha_i, \quad i = 1, 2.$$

In a similar way, from (3.3) and (3.6), we have

$$(3.11) \quad \sum_{i=1}^2 \frac{\gamma \alpha_i}{h} \|[\eta_i]\|_{0, \mathcal{E}_h}^2 \lesssim \gamma h^{2p} \|\alpha^{\frac{1}{2}} v\|_{p+1, \Omega_1 \cup \Omega_2}^2,$$



$$(3.12) \quad \sum_{i=1}^2 \frac{h}{\gamma \alpha_i} \|\{\alpha_i \nabla \eta_i \cdot \mathbf{n}\}\|_{0, \mathcal{E}_h^i}^2 \lesssim \frac{1}{\gamma} h^{2p} \|\alpha^{\frac{1}{2}} v\|_{p+1, \Omega_1 \cup \Omega_2}^2.$$

Now the proof of the lemma follows by combining (3.7)–(3.12).  $\square$

Note that the bound of the interpolation error in the above lemma depends on the full norm of  $v$  in  $H^{p+1}(\Omega_1 \cup \Omega_2)$ . However, we expect the seminorm of  $v$  in the error estimates, to agree with the classical theory of FEM on non-interfacial elliptic problems. The following lemma points out that the error of best approximation from  $V_h$  for any  $v \in V$  is indeed controlled by the seminorm of  $v$ .

**Lemma 3.5.** *Suppose  $0 < h \leq h_0$ . Then*

$$\inf_{v_h \in V_h} \|v - v_h\|_h \lesssim (1 + \gamma + \gamma^{-1})^{\frac{1}{2}} h^p |\alpha^{\frac{1}{2}} v|_{p+1, \Omega_1 \cup \Omega_2}, \quad \forall v \in \{v \in H^{p+1}(\Omega_1 \cup \Omega_2) : v|_{\partial\Omega} = 0\}.$$

*Proof.* Denote by  $\mathcal{Q}_p(\Omega_1 \cup \Omega_2) = \{q : q|_{\Omega_i} = q_i|_{\Omega_i}, q_i \in \mathcal{Q}_p(\Omega_i), i = 1, 2\}$ . Noting that  $v_h = I_h(v + q) - q \in V_h$  for any  $q \in \mathcal{Q}_p(\Omega_1 \cup \Omega_2)$ , we have from Lemmas 3.4 and 3.3 that

$$\begin{aligned} \inf_{v_h \in V_h} \|v - v_h\|_h &\lesssim \inf_{q \in \mathcal{Q}_p(\Omega_1 \cup \Omega_2)} \|v + q - I_h(v + q)\|_h \\ &\lesssim (1 + \gamma + \gamma^{-1})^{\frac{1}{2}} h^p \inf_{q \in \mathcal{Q}_p(\Omega_1 \cup \Omega_2)} \|\alpha^{\frac{1}{2}}(v + q)\|_{p+1, \Omega_1 \cup \Omega_2} \\ &\lesssim (1 + \gamma + \gamma^{-1})^{\frac{1}{2}} h^p \left( \sum_{i=1}^2 \alpha_i \inf_{q_i \in \mathcal{Q}_p(\Omega_i)} \|v + q_i\|_{p+1, \Omega_i}^2 \right)^{\frac{1}{2}} \\ &\lesssim (1 + \gamma + \gamma^{-1})^{\frac{1}{2}} h^p |\alpha^{\frac{1}{2}} v|_{p+1, \Omega_1 \cup \Omega_2}. \end{aligned}$$

This completes the proof of the lemma.  $\square$

### 3.1 $H^1$ error estimate

Next, we give the continuity and coercivity of the bilinear form  $a_h(\cdot, \cdot)$  in the following lemma.

**Lemma 3.6.** *We have*

$$(3.13) \quad |a_h(u, v)| \leq 2 \|u\|_h \|v\|_h, \quad \forall u, v \in V.$$

*Suppose  $0 < h \leq h_0$ . Then there exists a constant  $\gamma_0 > 0$  independent of  $h$ , the coefficient  $\alpha$ , and the mesh  $\mathcal{M}_h$ , such that, for  $\gamma \geq \gamma_0$*

$$(3.14) \quad a_h(v_h, v_h) \geq \frac{1}{2} \|v_h\|_h^2, \quad \forall v_h \in V_h,$$

*where the constant  $h_0$  is from Lemma 3.1.*

*Proof.* (3.13) follows from the Cauchy-Schwarz inequality. It remains to prove (3.14). From (2.6) and (2.12),

$$\begin{aligned}
a_h(v_h, v_h) &= \|v_h\|_h^2 - 2(\{\alpha \nabla v_h \cdot \mathbf{n}\}_w, [v_h])_\Gamma - \frac{h}{\gamma \{\alpha\}_w} \|\{\alpha \nabla v_h \cdot \mathbf{n}\}_w\|_{0,\Gamma}^2 \\
&\quad - 2 \sum_{i=1}^2 (\{\alpha_i \nabla v_h \cdot \mathbf{n}\}, [v_h])_{\mathcal{E}_h^i} - \sum_{i=1}^2 \frac{h}{\gamma \alpha_i} \|\{\alpha_i \nabla v \cdot \mathbf{n}\}\|_{0,\mathcal{E}_h^i}^2 \\
&\geq \|v_h\|_h^2 - \frac{1}{2} \frac{\gamma \{\alpha\}_w}{h} \| [v_h] \|_{0,\Gamma}^2 - 3 \frac{h}{\gamma \{\alpha\}_w} \|\{\alpha \nabla v_h \cdot \mathbf{n}\}_w\|_{0,\Gamma}^2 \\
&\quad - \frac{1}{2} \sum_{i=1}^2 \frac{\gamma \alpha_i}{h} \| [v_h] \|_{0,\mathcal{E}_h^i}^2 - 3 \sum_{i=1}^2 \frac{h}{\gamma \alpha_i} \|\{\alpha_i \nabla v_h \cdot \mathbf{n}\}\|_{0,\mathcal{E}_h^i}^2.
\end{aligned}$$

On the other hand, from (3.2) and (3.10) we deduce that

$$\begin{aligned}
3 \frac{h}{\gamma \{\alpha\}_w} \|\{\alpha \nabla v_h \cdot \mathbf{n}\}_w\|_{0,\Gamma}^2 &\leq 6 \sum_{i=1}^2 \sum_{K \in \mathcal{M}_{h,i}^\Gamma} \frac{h}{\gamma \{\alpha\}_w} \|\alpha_i w_i \nabla(v_h|_{\Omega_i})\|_{0,K \cap \Omega}^2 \\
&\leq 6 \sum_{i=1}^2 \sum_{K \in \mathcal{M}_{h,i}^\Gamma} \frac{\alpha_i^2 w_i^2}{\gamma \{\alpha\}_w} C_{tr1}^2 \|\nabla v_h\|_{0,K \cap \Omega_i}^2 \\
&\leq \frac{3C_{tr1}^2}{\gamma} \sum_{i=1}^2 \sum_{K \in \mathcal{M}_{h,i}^\Gamma} \alpha_i \|\nabla v_h\|_{0,K \cap \Omega_i}^2 \\
&\leq \frac{3C_{tr1}^2}{\gamma} \|\alpha^{\frac{1}{2}} \nabla v_h\|_{0,\Omega_1 \cup \Omega_2}^2.
\end{aligned}$$

(3.15)

Analogously, from (3.4) we have

$$(3.16) \quad 3 \sum_{i=1}^2 \frac{h}{\gamma \alpha_i} \|\{\alpha \nabla v_h \cdot \mathbf{n}\}\|_{0,\mathcal{E}_h^i}^2 \leq \frac{3C_{tr2}^2}{2\gamma} \|\alpha^{\frac{1}{2}} \nabla v_h\|_{0,\Omega_1 \cup \Omega_2}^2.$$

By combining the above three estimates, we have

$$a_h(v_h, v_h) \geq \|v_h\|_h^2 - \max\left\{\frac{1}{2}, \frac{3C_{tr1}^2}{\gamma}, \frac{3C_{tr2}^2}{2\gamma}\right\} \|v_h\|_h^2.$$

Then (3.14) follows by taking  $\gamma_0 = \max\{6C_{tr1}^2, 3C_{tr2}^2\}$ , where the constant  $C_{tr1}$  and  $C_{tr2}$  is from (3.2) and (3.4). This completes the proof of the lemma.  $\square$

The following Céa lemma says that the error of the discrete solution can be bounded by the error of the best approximation from  $V_h$ .

**Lemma 3.7.** *Suppose  $0 < h \leq h_0$  and  $\gamma \geq \gamma_0$ . Then*

$$\|u - u_h\|_h \leq 5 \inf_{v_h \in V_h} \|u - v_h\|_h.$$

*Proof.* For any  $v_h \in V_h$ , let  $\eta_h = u_h - v_h$ . From (2.11) and Lemma 3.6,

$$\|\eta_h\|_h^2 \leq 2a_h(\eta_h, \eta_h) = 2a_h(u - v_h, \eta_h) \leq 4 \|u - v_h\|_h \|\eta_h\|_h.$$

Therefore,

$$\|u_h - v_h\|_h \leq 4 \|u - v_h\|_h,$$

which implies

$$\|u - u_h\|_h = \|u - v_h + v_h - u_h\|_h \leq 5 \|u - v_h\|_h.$$

This completes the proof of the lemma.  $\square$

The following  $H^1$ -error estimate is a direct consequence of Lemma 3.5 and Lemma 3.7. The proof is omitted.

**Theorem 3.1.** *Suppose  $0 < h \leq h_0$ ,  $\gamma \geq \gamma_0$ , and the solution to the interface problem (2.1) satisfies  $u \in H^{p+1}(\Omega_1 \cup \Omega_2)$ . Then there holds the following error estimate*

$$(3.17) \quad \|u - u_h\|_h \lesssim \gamma^{\frac{1}{2}} h^p |\alpha^{\frac{1}{2}} u|_{p+1, \Omega_1 \cup \Omega_2}.$$

**Remark 3.1.** *From the definition (2.12) of  $\|\cdot\|_h$ , the above theorem implies the following estimates.*

$$(3.18) \quad \|\alpha^{\frac{1}{2}} \nabla(u - u_h)\|_{0, \Omega_1 \cup \Omega_2} \lesssim \gamma^{\frac{1}{2}} h^p |\alpha^{\frac{1}{2}} u|_{p+1, \Omega_1 \cup \Omega_2},$$

$$(3.19) \quad \{\alpha\}_w^{\frac{1}{2}} \|[u_h] - g_D\|_{0, \Gamma} \lesssim h^{p+\frac{1}{2}} |\alpha^{\frac{1}{2}} u|_{p+1, \Omega_1 \cup \Omega_2}.$$

*The first inequality gives convergence rate of the error in energy norm and the second one gives convergence rate of the first interface condition  $[u] = g_D$ . The convergence rate of the second interface condition can also be derived but we leave it for the interested readers.*

### 3.2 $L^2$ error estimate

Next we prove the  $L^2$ -error estimate by using the Aubin-Nitsche trick.

**Theorem 3.2.** *Under the same conditions of Theorem 3.1, there holds*

$$\|u - u_h\|_{0, \Omega} \lesssim \gamma h^{p+1} \alpha_{\min}^{-\frac{1}{2}} |\alpha^{\frac{1}{2}} u|_{p+1, \Omega_1 \cup \Omega_2}.$$

*Proof.* Let  $\varphi$  be the solution of the following auxiliary problem

$$(3.20) \quad \begin{cases} -\nabla \cdot (\alpha \nabla \varphi) = u - u_h & \text{in } \Omega_1 \cup \Omega_2, \\ [\varphi] = 0, \quad [(\alpha \nabla \varphi) \cdot \mathbf{n}] = 0 & \text{on } \Gamma, \\ \varphi = 0 & \text{on } \partial\Omega. \end{cases}$$

The solution enjoys the following regularity estimate (cf. [25]):

$$(3.21) \quad |\alpha \varphi|_{j, \Omega_1 \cup \Omega_2} \lesssim \|u - u_h\|_{0, \Omega}, \quad j = 1, 2.$$

Therefore, from Lemma 3.5,

$$(3.22) \quad \inf_{\varphi_h \in V_h} \|\varphi - \varphi_h\|_h \lesssim \gamma^{\frac{1}{2}} h |\alpha^{\frac{1}{2}} \varphi|_{2, \Omega_1 \cup \Omega_2} \lesssim \gamma^{\frac{1}{2}} \alpha_{\min}^{-\frac{1}{2}} h \|u - u_h\|_{0, \Omega}.$$

Set  $\eta = u - u_h$ , testing (3.20) by  $\eta$  and using (2.11), (3.13), and (3.22), we get

$$\begin{aligned} \|\eta\|_{0, \Omega}^2 &= a_h(u - u_h, \varphi) = \inf_{\varphi_h \in V_h} a_h(u - u_h, \varphi - \varphi_h) \\ &\leq 2 \|u - u_h\|_h \inf_{\varphi_h \in V_h} \|\varphi - \varphi_h\|_h \\ &\lesssim \|u - u_h\|_h \gamma^{\frac{1}{2}} \alpha_{\min}^{-\frac{1}{2}} h \|u - u_h\|_{0, \Omega}, \end{aligned}$$

that is

$$\|\eta\|_{0, \Omega} \lesssim \gamma^{\frac{1}{2}} \alpha_{\min}^{-\frac{1}{2}} h \|u - u_h\|_h,$$

which completes the proof by using Theorem 3.1.  $\square$

**Remark 3.2.** *With analogous tricks to SUIPDG-FEM, we can also obtain the optimal energy error estimate for NUIPDG-FEM ( $\beta = -1$ ), even with a broader requirement for the penalty parameter  $\gamma$ . Suppose  $0 < h \leq h_0$ ,  $\gamma \gtrsim 1$ ,  $\beta = -1$ , and the solution to the interface problem (2.1) satisfies  $u \in H^{p+1}(\Omega_1 \cup \Omega_2)$ . Then there holds the following error estimate*

$$\|u - u_h\|_h \lesssim \gamma^{\frac{1}{2}} h^p |\alpha^{\frac{1}{2}} u|_{p+1, \Omega_1 \cup \Omega_2}.$$

However, the nonsymmetric formulation is not adjoint consistent and the  $L^2$ -error estimate is suboptimal for the NUIPDG-FEM by an order in  $h$ , it is same with IPDG method for elliptic problem without interface. Under the above conditions, we have:

$$\|u - u_h\|_{0, \Omega} \lesssim (\alpha_{\min}^{-\frac{1}{2}} \gamma h^{p+1} + h^{p+\frac{1}{2}} + \alpha_{\min}^{-\frac{1}{2}} h^p) |\alpha^{\frac{1}{2}} u|_{p+1, \Omega_1 \cup \Omega_2}.$$

### 3.3 Flux error estimate

One may be interested in the approximation error of the flux  $\alpha \nabla u_h$ . For the treatment of the flux  $\alpha \nabla u_h$ , we need a discrete extension operator  $\mathfrak{E}_{h,i}$  mapping  $V_{h,i}$  onto  $V_h$ . In [9], a linear and continuous case is considered, and [26] extend this result to higher order elements. On the basis, we construct a kind of discrete extension operator for UIPDG-FEM.

**Lemma 3.8.** *There exists a positive constant  $h_0$  depending only on the interface  $\Gamma$  and the shape regularity of the meshes, such that for all  $h \in (0, h_0)$  and  $i = 1$  or  $2$ , there exists a discrete extension operator  $\mathfrak{E}_{h,i} : V_{h,i} \mapsto V_h$ , which satisfies: for any  $v_{h,i} \in V_{h,i}$ ,  $\mathfrak{E}_{h,i} v_{h,i} \in V_h$ ,  $\mathfrak{E}_{h,i} v_{h,i}$  is only different from  $v_{h,i}$  in  $\Omega_i$  by a constant  $C$ ,  $\mathfrak{E}_{h,i} v_{h,i}$  is continuous in  $\Omega_{3-i}$  and*

$$(3.23) \quad \|\mathfrak{E}_{h,i} v_{h,i}\|_{0, \Gamma} \leq C_{\Gamma} \|v_{h,i}\|_{0, \mathcal{E}_h^i}, \quad \|\nabla \mathfrak{E}_{h,i} v_{h,i}\|_{0, \Omega}^2 \leq C_{\Omega_i}^2 (\|\nabla v_{h,i}\|_{0, \Omega_i}^2 + \frac{1}{h} \|v_{h,i}\|_{\mathcal{E}_h^i}^2).$$

*Proof.* Let  $\{x_j\}_{j=1}^J$  be the set of nodal points of the space  $U_h \cdot \chi_{\Omega_{h,i}}$  and  $\{\psi_j\}_{j=1}^J$  the corresponding nodal basis functions. Firstly, we interpolate  $v_{h,i}$  in the continuous space  $U \cdot \chi_{\Omega_{h,i}}$ . Actually, we

take the average value on  $x_j$  when the nodal point is shared by several elements. This way, we construct an interpolant  $I_{h,i} : V_{h,i} \mapsto U_h \cdot \chi_{\Omega_{h,i}}$ ,

$$(I_{h,i}v_{h,i})(x) = \sum_{j=1}^J \overline{v_{h,i}(x_j)} \psi_j(x), \quad \forall v_{h,i} \in V_{h,i}.$$

Note that  $I_{h,i}v_{h,i}$  is continuous in  $\Omega_i$  and is only different from  $v_{h,i}$  on  $\mathcal{E}_h^i$ . It is easy to check that

$$\|\nabla I_{h,i}v_{h,i}\|_{0,\Omega_i}^2 \leq \|\nabla v_{h,i}\|_{0,\Omega_i}^2 + \frac{1}{h} \|[v_{h,i}]\|_{0,\mathcal{E}_h^i}^2.$$

We take  $z_h = I_{h,i}v_{h,i} - C$ , where  $C = 0$  if  $\partial\Omega_i \cap \partial\Omega \neq \emptyset$  and  $C = \frac{1}{|\Omega_i|} \int_{\Omega_i} I_{h,i}v_{h,i}$  otherwise. By [26, Lemma.3.3], one can find a discrete extension operator  $E_{h,i} : U_h \cdot \chi_{\Omega_{h,i}} \mapsto U_h$  and

$$E_{h,i}z_h = z_h \text{ in } \Omega_{h,i}, \quad \|E_{h,i}z_h\|_{1,\Omega} \leq C_{\Omega_i} \|z_h\|_{1,\Omega_i} = \|\nabla I_{h,i}v_{h,i}\|_{0,\Omega_i}.$$

The needed extension  $\mathfrak{E}_{h,i} : V_{h,i} \mapsto V_h$  is then defined as

$$\mathfrak{E}_{h,i}v_{h,i} = (v_{h,i} - C) \cdot \chi_{\Omega_i} + E_{h,i}z_h \cdot \chi_{\Omega_{3-i}}.$$

Clearly,  $\mathfrak{E}_{h,i}v_{h,i}$  is continuous in  $\Omega_{3-i}$ , and

$$\|[\mathfrak{E}_{h,i}v_{h,i}]\|_{0,\Gamma}^2 \leq C_{\Gamma} h^{d-1} \|v_{h,i} - I_{h,i}v_{h,i}\|_{\infty,\mathcal{E}_h^i}^2 \leq C_{\Gamma} \|[v_{h,i}]\|_{0,\mathcal{E}_h^i}^2$$

□

We can now use the above theorem together with the trick from [9] to derive the following theorem, of which the special high-order discrete extension operator in (3.23) plays an important role in the proof.

**Theorem 3.3.** *Suppose  $0 < h \leq h_0$ ,  $\gamma \geq \gamma_0$ , and the solution to the interface problem (2.1) satisfies  $u \in H^{p+1}(\Omega_1 \cup \Omega_2)$ . Then there holds the following error estimate*

$$(3.24) \quad \|\alpha \nabla(u - u_h)\|_{0,\Omega_1 \cup \Omega_2} \lesssim \gamma^{\frac{1}{2}} h^p |\alpha u|_{p+1,\Omega_1 \cup \Omega_2}.$$

*Proof.* Without loss of generality, we assume  $\alpha_2 \geq \alpha_1$ . Thus, the estimate of (3.24) in  $\Omega_1$  is implied by (3.18) since

$$(3.25) \quad \|\alpha_1 \nabla(u - u_h)\|_{0,\Omega_1} = \alpha_1^{\frac{1}{2}} \|\alpha_1^{\frac{1}{2}} \nabla(u - u_h)\|_{0,\Omega_1} \lesssim \gamma^{\frac{1}{2}} h^p |\alpha u|_{p+1,\Omega_1 \cup \Omega_2}.$$

To bound  $\|\alpha_2 \nabla(u - u_h)\|_{0,\Omega_2}$ , we resort to the discrete extension operator  $\mathfrak{E}_h := \mathfrak{E}_{h,2}$  defined in Lemma 3.8. We substitute  $v_h = \mathfrak{E}_h(u_h - I_h u)$  in (2.11) and multiply both sides by  $\alpha_2$  to obtain

that

$$\begin{aligned}
& \alpha_2^2 \|\nabla(u_h - I_h u)\|_{0,\Omega_2}^2 + \frac{\gamma \alpha_2^2}{h} \|[u_h - I_h u]\|_{0,\mathcal{E}_h^2}^2 \\
&= \alpha_2 \int_{\Omega_1 \cup \Omega_2} \alpha \nabla(u - I_h u) \cdot \nabla v_h - \alpha_2 \int_{\Omega_1} \alpha_1 \nabla(u_h - I_h u) \cdot \nabla v_h \\
&\quad - \alpha_2 \int_{\Gamma} (\{\alpha \nabla(u - u_h) \cdot \mathbf{n}\}_w [v_h] + [u - u_h] \{\alpha \nabla v_h \cdot \mathbf{n}\}_w) \\
&\quad - \alpha_2^2 \int_{\mathcal{E}_h^2} (\{\nabla(u - u_h) \cdot \mathbf{n}\} [v_h] + [u - u_h] \{\nabla v_h \cdot \mathbf{n}\}) - \alpha_1 \alpha_2 \int_{\mathcal{E}_h^1} [u - u_h] \{\nabla v_h \cdot \mathbf{n}\} \\
(3.26) \quad &+ \frac{\gamma \alpha_2^2}{h} \int_{\mathcal{E}_h^2} [u - I_h u] [v_h] + \frac{\gamma \{\alpha\}_w \alpha_2}{h} \int_{\Gamma} [u - u_h] [v_h].
\end{aligned}$$

Here we have used the fact that  $v_h$  is continuous in  $\Omega_1$ , so the terms involving  $[v_h]$  within  $\Omega_1$  vanish.

Using the inequality  $ab \leq \varepsilon a^2 + \frac{b^2}{4\varepsilon}$ ,  $\forall \varepsilon > 0$ , we can bound the terms on the right-hand side of (3.26) as follows

$$\begin{aligned}
& \alpha_2 \int_{\Omega_1 \cup \Omega_2} \alpha \nabla(u - I_h u) \cdot \nabla v_h \leq \varepsilon \alpha_2^2 \|\nabla v_h\|_{0,\Omega}^2 + \frac{1}{4\varepsilon} \|\alpha \nabla(u - I_h u)\|_{0,\Omega_1 \cup \Omega_2}^2 \\
&\quad \leq \varepsilon C_{\Omega_2}^2 \alpha_2^2 (\|\nabla(u_h - I_h u)\|_{0,\Omega_2}^2 + \frac{1}{h} \|[u_h - I_h u]\|_{0,\mathcal{E}_h^2}^2) + \frac{1}{4\varepsilon} \|\alpha \nabla(u - I_h u)\|_{0,\Omega_1 \cup \Omega_2}^2, \\
& \alpha_2 \int_{\Omega_1} \alpha_1 \nabla(u_h - I_h u) \cdot \nabla v_h \leq \varepsilon \alpha_2^2 \|\nabla v_h\|_{0,\Omega_1}^2 + \frac{1}{4\varepsilon} \|\alpha_1 \nabla(u_h - I_h u)\|_{0,\Omega_1}^2 \\
&\quad \leq \varepsilon C_{\Omega_2}^2 \alpha_2^2 (\|\nabla(u_h - I_h u)\|_{0,\Omega_2}^2 + \frac{1}{h} \|[u_h - I_h u]\|_{0,\mathcal{E}_h^2}^2) + \frac{1}{4\varepsilon} \|\alpha_1 \nabla(u_h - I_h u)\|_{0,\Omega_1}^2, \\
& \alpha_2 \int_{\Gamma} [u - u_h] \{\alpha \nabla v_h \cdot \mathbf{n}\}_w \leq \varepsilon h \alpha_2^2 \|\{\nabla v_h \cdot \mathbf{n}\}\|_{0,\Gamma}^2 + \frac{\{\alpha\}_w^2}{4\varepsilon h} \|[u - u_h]\|_{0,\Gamma}^2 \\
&\quad \leq \varepsilon C_{tr1}^2 C_{\Omega_2}^2 \alpha_2^2 (\|\nabla(u_h - I_h u)\|_{0,\Omega_2}^2 + \frac{1}{h} \|[u_h - I_h u]\|_{0,\mathcal{E}_h^2}^2) + \frac{\{a\}_w}{4\varepsilon \gamma} \|u - u_h\|_h^2, \\
& \alpha_2 \int_{\Gamma} \{\alpha \nabla(u - u_h) \cdot \mathbf{n}\}_w [v_h] \leq \frac{\varepsilon \gamma \alpha_2^2}{h} \|[v_h]\|_{0,\Gamma}^2 + \frac{h}{4\varepsilon \gamma} \|\{\alpha \nabla(u - u_h) \cdot \mathbf{n}\}_w\|_{0,\Gamma}^2 \\
&\quad \leq \frac{\varepsilon C_{\Gamma}^2 \gamma \alpha_2^2}{h} \|[u_h - I_h u]\|_{0,\mathcal{E}_h^2}^2 + \frac{\{a\}_w}{4\varepsilon} \|u - u_h\|_h^2, \\
& \alpha_2^2 \int_{\mathcal{E}_h^2} \{\nabla(u - u_h) \cdot \mathbf{n}\} [v_h] \leq \varepsilon h \alpha_2^2 \|\{\nabla(u - u_h) \cdot \mathbf{n}\}\|_{0,\mathcal{E}_h^2}^2 + \frac{\alpha_2^2}{4\varepsilon h} \|[v_h]\|_{0,\mathcal{E}_h^2}^2 \\
&\quad \leq \varepsilon \alpha_2^2 C_{tr2}^2 \|\nabla(u - I_h u)\|_{0,\Omega_2}^2 + \varepsilon \alpha_2^2 C_{tr2}^2 \|\nabla(u_h - I_h u)\|_{0,\Omega_2}^2 + \frac{\alpha_2^2}{4\varepsilon h} \|[v_h]\|_{0,\mathcal{E}_h^2}^2, \\
& \alpha_2^2 \int_{\mathcal{E}_h^2} [u - u_h] \{\nabla v_h \cdot \mathbf{n}\} \leq \varepsilon \alpha_2^2 h \|\{\nabla v_h \cdot \mathbf{n}\}\|_{0,\mathcal{E}_h^2}^2 + \frac{\alpha_2^2}{4\varepsilon h} \|[u - u_h]\|_{0,\mathcal{E}_h^2}^2 \\
&\quad \leq \varepsilon \alpha_2^2 C_{tr2}^2 \|\nabla(u_h - I_h u)\|_{0,\Omega_2}^2 + \frac{\alpha_2^2}{4\varepsilon h} (\|[u - I_h u]\|_{0,\mathcal{E}_h^2}^2 + \|[u_h - I_h u]\|_{0,\mathcal{E}_h^2}^2).
\end{aligned}$$

The similar arguments can apply to the other items. Combining the above estimates with the identity (3.26) and (3.6), (3.25), (3.18), (3.17), (2.5), we deduce that

$$\begin{aligned} & \left(1 - \varepsilon \left( \frac{2C_{\Omega_2}^2 + C_{tr1}^2 C_{\Omega_2}^2}{\gamma} + 2C_{\Gamma}^2 + 1 \right) - \frac{1}{2\varepsilon\gamma} \right) \frac{\gamma\alpha_2^2}{h} \|[u_h - I_h u]\|_{0,\mathcal{E}_h^2}^2 \\ & + (1 - 2\varepsilon(C_{\Omega_2}^2 + C_{tr2}^2 + C_{tr1}^2 C_{\Omega_2}^2))\alpha_2^2 \|\nabla(u_h - I_h u)\|_{0,\Omega_2}^2 \lesssim \gamma^{\frac{1}{2}} h^p |\alpha_2 u|_{p+1,\Omega_1 \cup \Omega_2} \end{aligned}$$

If  $\gamma$  is sufficiently large, and taking  $\varepsilon = \frac{1}{4(C_{\Omega_2}^2 + C_{tr2}^2 + C_{tr1}^2 C_{\Omega_2}^2 + C_{\Gamma}^2 + 1)}$ , we have

$$\|\alpha_2 \nabla(u_h - I_h u)\|_{0,\Omega_2} \lesssim \gamma^{\frac{1}{2}} h^p |\alpha_2 u|_{p+1,\Omega_1 \cup \Omega_2}.$$

Therefore, the error estimate for  $\|\alpha_2 \nabla(u - u_h)\|_{0,\Omega_2}$  follows from (3.6) and the triangle inequality. This completes the estimate of (3.24).  $\square$

**Remark 3.3.** (i) In the same way, the above results for the flux is also true for  $\beta \neq 1$ .

(ii) When  $g_D = g_N = 0$ . Under certain conditions, there holds the following regularity estimates for the interface problem [15, 25]:

$$|\alpha u|_{s+2,\Omega_1 \cup \Omega_2} \lesssim \|f\|_{s,\Omega_1 \cup \Omega_2}, \quad -1 \leq s \leq p-1.$$

Therefore, (3.24) gives the following error bound for the flux independent of the jump of the coefficient:

$$\|\alpha \nabla(u - u_h)\|_{0,\Omega_1 \cup \Omega_2} \lesssim \gamma^{\frac{1}{2}} h^p.$$

On the other hand, for the general  $g_D$  and  $g_N$ , (3.18) implies that

$$\frac{|\alpha^{\frac{1}{2}}(u - u_h)|_{1,\Omega_1 \cup \Omega_2}}{|\alpha^{\frac{1}{2}}u|_{1,\Omega_1 \cup \Omega_2}} \lesssim \gamma^{\frac{1}{2}} h^p \frac{|\alpha^{\frac{1}{2}}u|_{p+1,\Omega_1 \cup \Omega_2}}{|\alpha^{\frac{1}{2}}u|_{1,\Omega_1 \cup \Omega_2}} \lesssim \gamma^{\frac{1}{2}} h^p.$$

That is, the relative error in the energy norm is independent of the jump of the coefficient as well as the relative position of the interface to the mesh.

Furthermore, when  $g_D \neq 0$ ,  $g_N \neq 0$ , we also have the following regularity estimates for the interface problem:

**Theorem 3.4.** Suppose that both the boundary  $\partial\Omega$  and the interface  $\Gamma$  are smooth and  $u \in H^s(\Omega_1 \cup \Omega_2)$  with  $s \geq 2$ , the interface problem (2.1) satisfies the following shift estimate,

$$(3.27) \quad |\alpha u|_{s,\Omega_1 \cup \Omega_2} \leq C(\|f\|_{s-2,\Omega_1 \cup \Omega_2} + \min\{\alpha_1, \alpha_2\} \|g_D\|_{s-\frac{1}{2},\Gamma} + \|g_N\|_{s-\frac{3}{2},\Gamma}).$$

*Proof.* We introduce an auxiliary function  $\tilde{u}$  to eliminate the inhomogeneous interface conditions, which is defined by distinguishing two cases, that is  $\alpha_1 \leq \alpha_2$  for **Case I** and  $\alpha_2 > \alpha_1$  for **Case II**.

In **Case I**, we first construct a  $\tilde{u}_1$  which solves

$$\begin{cases} \Delta^2 \tilde{u}_1 = 0 & \text{in } \Omega_1, \\ \tilde{u}_1 = g_D, \quad \alpha_1 \nabla \tilde{u}_1 \cdot \mathbf{n} = g_N & \text{on } \Gamma. \end{cases}$$

It is well-known that there exists a unique  $\tilde{u}_1$  to the above bi-harmonic problem satisfying the estimate [23],

$$(3.28) \quad \|\tilde{u}_1\|_{s,\Omega_1} \leq C \left( \|g_D\|_{s-\frac{1}{2},\Gamma} + \frac{1}{\alpha_1} \|g_N\|_{s-\frac{3}{2},\Gamma} \right).$$

We set  $\tilde{u}$  be the zero extension of  $\tilde{u}_1$  from  $\Omega_1$  to  $\Omega$  in this case.

While for **Case II**, we construct a  $\tilde{u}_2$  to solve

$$\begin{cases} \Delta^2 \tilde{u}_2 = 0 & \text{in } \Omega_2, \\ \tilde{u}_2 = -g_D, \quad \alpha_2 \nabla \tilde{u}_2 \cdot \mathbf{n} = -g_N & \text{on } \Gamma, \\ \tilde{u}_2 = 0, \quad \nabla \tilde{u}_2 \cdot \mathbf{n} = 0 & \text{on } \partial\Omega. \end{cases}$$

Similar to the estimate (3.28), we have

$$(3.29) \quad \|\tilde{u}_2\|_{s,\Omega_2} \leq C \left( \|g_D\|_{s-\frac{1}{2},\Gamma} + \frac{1}{\alpha_2} \|g_N\|_{s-\frac{3}{2},\Gamma} \right).$$

Let  $\tilde{u}$  be the zero extension of  $\tilde{u}_2$  from  $\Omega_2$  to  $\Omega$  in this case.

Next we set  $\hat{u} = u - \tilde{u}$  for both cases, then  $\hat{u}$  solves

$$\begin{cases} -\nabla \cdot (\alpha \nabla \hat{u}) = f + \nabla \cdot (\alpha \nabla \tilde{u}), & \text{in } \Omega, \\ [\hat{u}] = 0, \quad [\alpha \nabla \hat{u} \cdot \mathbf{n}] = 0, & \text{on } \Gamma, \\ \hat{u} = 0, & \text{on } \partial\Omega. \end{cases}$$

From the regularity estimate for homogeneous jump conditions [15], we have

$$|\alpha \hat{u}|_{s,\Omega_1 \cup \Omega_2} \leq C (\|f\|_{s-2,\Omega_1 \cup \Omega_2} + \|\alpha \Delta \tilde{u}\|_{s-2,\Omega_1 \cup \Omega_2}),$$

and hence

$$|\alpha u|_{s,\Omega_1 \cup \Omega_2} \leq C (\|f\|_{s-2,\Omega_1 \cup \Omega_2} + \|\alpha \tilde{u}\|_{s,\Omega_1 \cup \Omega_2}),$$

which together with (3.28)–(3.29) implies that (3.27) holds. This completes the proof of the theorem.  $\square$

**Remark 3.4.** *Theorems 3.3–3.4 show that the error bound for the flux are also independent of the jump of the coefficient when the jump condition is inhomogeneous.*

## 4 Estimate of the condition number

In this section, we will show that the condition number of the stiffness matrix satisfies a similar upper bound as the one resulting from a standard finite element method [18], which is independent of the relative position of the interface to the meshes. For simplicity, we consider only the symmetric version of the SUIPDG-FEM ( $\beta = 1$ ).



## 4.1 Three condition numbers

Denote by  $\mathcal{N}_{h,1} = \{z_1^1, z_1^2, \dots, z_1^{N_1}\}$  and by  $\mathcal{N}_{h,2} \setminus \partial\Omega = \{z_2^1, z_2^2, \dots, z_2^{N_2}\}$  the sets of nodal points for the induced meshes  $V_{h,1}$  and  $V_{h,2}$ , respectively. Then for any  $v_h \in V_h$ ,

$$(4.1) \quad \mathbf{v} = (v_h(z_1^1), v_h(z_1^2), \dots, v_h(z_1^{N_1}), v_h(z_2^1), v_h(z_2^2), \dots, v_h(z_2^{N_2}))$$

is the corresponding vector of degrees of freedom, and the stiffness matrix  $A$  and the mass matrix  $M$  are symmetric matrices given by

$$(4.2) \quad a_h(v_h, v_h) = \mathbf{v}^T A \mathbf{v} \quad \text{and} \quad (v_h, v_h) = \mathbf{v}^T M \mathbf{v},$$

respectively. Define the linear operator  $\mathcal{A}_h : V_h \mapsto V_h$  by

$$a_h(v_h, w_h) = (\mathcal{A}_h v_h, w_h), \quad \forall v_h, w_h \in V_h.$$

Then

$$(4.3) \quad \frac{\mathbf{v}^T A \mathbf{v}}{\mathbf{v}^T \mathbf{v}} = \frac{(\mathcal{A}_h v_h, v_h)}{(v_h, v_h)} \frac{\mathbf{v}^T M \mathbf{v}}{\mathbf{v}^T \mathbf{v}}, \quad \forall v_h \in V_h \setminus \{0\}.$$

Denote by  $\lambda_{max}^A, \lambda_{max}^M, \lambda_{max}^{\mathcal{A}_h}$  and  $\lambda_{min}^A, \lambda_{min}^M, \lambda_{min}^{\mathcal{A}_h}$  the maximum and minimum eigenvalues of  $A, M, \mathcal{A}_h$ , respectively. Then the condition numbers of  $A, M, \mathcal{A}_h$  satisfy

$$\kappa(A) = \frac{\lambda_{max}^A}{\lambda_{min}^A}, \quad \kappa(\mathcal{A}_h) = \frac{\lambda_{max}^{\mathcal{A}_h}}{\lambda_{min}^{\mathcal{A}_h}}, \quad \text{and} \quad \kappa(M) = \frac{\lambda_{max}^M}{\lambda_{min}^M}.$$

As a consequence of (4.3), we have

$$(4.4) \quad \kappa(A) \leq \kappa(\mathcal{A}_h) \kappa(M).$$

## 4.2 Estimate of $\kappa(\mathcal{A}_h)$

Inspired by [1, Lemma 2.1], we have the following Poincaré type inequality.

**Lemma 4.1.** *For all  $v \in V$ , we have*

$$(4.5) \quad \|v\|_{0,\Omega} \lesssim \|\nabla v\|_{0,\Omega_1 \cup \Omega_2} + \|[v]\|_{0,\Gamma} + h^{-\frac{1}{2}} \left( \sum_{i=1}^2 \|[v]\|_{0,\mathcal{E}_h^i}^2 \right)^{\frac{1}{2}}.$$

*Proof.* Let  $w$  be the solution of the following problem,

$$(4.6) \quad \begin{cases} -\Delta w = v, & \text{in } \Omega \\ w = 0, & \text{on } \partial\Omega \end{cases}$$

The solution enjoys the following regularity estimate(cf. [16])

$$(4.7) \quad \|w\|_{H^2} \lesssim \|v\|_{L^2}.$$

Test (4.6) by  $v$ , we have

$$\begin{aligned}
\|v\|_{0,\Omega}^2 &= \sum_{i=1}^2 \sum_{K \in \mathcal{M}_{h,i}} \left( \int_{K \cap \Omega_i} \nabla w \cdot \nabla v - \int_{\partial(K \cap \Omega_i)} \nabla w \cdot \mathbf{n} v \right) \\
&\lesssim \|\nabla w\|_{0,\Omega_1 \cup \Omega_2} \|\nabla v\|_{0,\Omega_1 \cup \Omega_2} + \sum_{i=1}^2 (\nabla w \cdot \mathbf{n}, [v])_{\mathcal{E}_h^i} + (\nabla w \cdot \mathbf{n}, [v])_{\Gamma} \\
&\lesssim \|\nabla w\|_{0,\Omega_1 \cup \Omega_2} \|\nabla v\|_{0,\Omega_1 \cup \Omega_2} + \sum_{i=1}^2 h^{\frac{1}{2}} \|\nabla w\|_{0,\mathcal{E}_h^i} h^{-\frac{1}{2}} \|[v]\|_{0,\mathcal{E}_h^i} + \|\nabla w\|_{0,\Gamma} \|[v]\|_{0,\Gamma} \\
&\lesssim \|\nabla w\|_{0,\Omega_1 \cup \Omega_2} \|\nabla v\|_{0,\Omega_1 \cup \Omega_2} + \|\nabla w\|_{0,\Gamma} \|[v]\|_{0,\Gamma} \\
(4.8) \quad &+ h^{-\frac{1}{2}} (\|\nabla w\|_{0,\Omega_1 \cup \Omega_2} + h \|\nabla w\|_{1,\Omega_1 \cup \Omega_2}) \left( \sum_{i=1}^2 \|[v]\|_{0,\mathcal{E}_h^i}^2 \right)^{\frac{1}{2}}
\end{aligned}$$

Then the proof of lemma follows by combining (4.7) and (4.8).  $\square$

Next, we derive an inverse inequality in  $V_h$ .

**Lemma 4.2.** *Suppose  $0 < h \leq h_0$ . Then*

$$(4.9) \quad \|v_h\|_h \lesssim (\gamma^{-\frac{1}{2}} + \gamma^{\frac{1}{2}}) h^{-1} \|\alpha^{\frac{1}{2}} v_h\|_{0,\Omega}, \quad \forall v_h \in V_h.$$

*Proof.* It follows from (2.12), (3.15) and (3.16) that

$$\|v_h\|_h^2 \lesssim (1 + \gamma^{-1}) \|\alpha^{\frac{1}{2}} \nabla v_h\|_{0,\Omega_1 \cup \Omega_2}^2 + \frac{\gamma \{\alpha\}_w}{h} \|[v_h]\|_{0,\Gamma}^2 + \sum_{i=1}^2 \frac{\gamma \alpha_i}{h} \|[v_h]\|_{0,\mathcal{E}_h^i}^2.$$

Therefore, from the inverse inequality, (3.3) and  $\{\alpha\}_w \lesssim \alpha_i, i = 1, 2$ ,

$$\|v_h\|_h^2 \lesssim (1 + \gamma^{-1}) h^{-2} \|\alpha^{\frac{1}{2}} v_h\|_{0,\Omega_1 \cup \Omega_2}^2 + \gamma \sum_{i=1}^2 h^{-2} \alpha_i \|v_h\|_{0,\Omega_i}^2.$$

That is, (4.9) holds. This completes the proof of the lemma.  $\square$

The following lemma gives an estimate for  $\kappa(\mathcal{A}_h)$ .

**Lemma 4.3.** *Suppose  $\gamma_0 \leq \gamma \lesssim 1$  and  $0 < h \leq h_0$ . Then*

$$\kappa(\mathcal{A}_h) \lesssim \frac{\alpha_{max}}{\alpha_{min}} \frac{1}{h^2}.$$

*Proof.* Lemma 3.6 implies that

$$\|v_h\|_h^2 \lesssim a_h(v_h, v_h) \lesssim \|v_h\|_h^2, \quad \forall v_h \in V_h.$$

From Lemma 4.1, (2.12), and (2.5)

$$\|v_h\|_{0,\Omega}^2 \lesssim \alpha_{min}^{-1} (1 + \gamma^{-1} h) \|v_h\|_h^2, \quad \forall v_h \in V_h.$$

Therefore, Lemma 4.2 and the above two estimates give

$$\lambda_{min}^{\mathcal{A}_h} \gtrsim \alpha_{min} (1 + \gamma^{-1} h)^{-1} \quad \text{and} \quad \lambda_{max}^{\mathcal{A}_h} \lesssim \alpha_{max} (\gamma^{-1} + \gamma) h^{-2},$$

which imply that the lemma holds.  $\square$

### 4.3 Estimate of $\kappa(M)$

Clearly, for any  $v_h \in V_h$ , there exists  $v_{h,i} \in V_{h,i}$  such that  $v_h|_{\Omega_i} = v_{h,i}|_{\Omega_i}$ ,  $i = 1, 2$ .

**Lemma 4.4.**

$$(4.10) \quad \sum_{i=1}^2 \|v_{h,i}\|_{0,\Omega_{h,i}} \lesssim \|v_h\|_{0,\Omega} \leq \sum_{i=1}^2 \|v_{h,i}\|_{0,\Omega_{h,i}}, \quad \forall v_h \in V_h,$$

*Proof.* The second inequality is obvious, it suffices to prove the first one that

$$\|v_{h,i}\|_{0,K} \lesssim \|v_{h,i}\|_{0,K \cap \Omega_i}, \quad \forall K \in \mathcal{M}_{h,i}^\Gamma.$$

□

**Lemma 4.5.** *The condition number of the mass matrix satisfies*

$$\kappa(M) \lesssim 1.$$

*Proof.* Denote by  $\mathbf{v}$  the vector of global degrees of freedom on  $V_h$ , due to norm equivalence on  $V_h$ , we have

$$\sum_{i=1}^2 \|v_{h,i}\|_{0,\Omega_{h,i}} \approx h^d(\mathbf{v}, \mathbf{v}).$$

Following from Lemma 4.5, proof of this lemma is completed. □

### 4.4 Estimate of $\kappa(A)$

The following theorem gives an estimate of the spectral condition number of the stiffness matrix.

**Theorem 4.1.** *Suppose  $\gamma_0 \leq \gamma \lesssim 1$  and  $0 < h \leq h_0$ . Then*

$$(4.11) \quad \kappa(A) \lesssim \frac{\alpha_{max}}{\alpha_{min}} \frac{1}{h^2}.$$

*Proof.* The proof follows by combining (4.4), Lemma 4.3, and Lemma 4.5. □

## 5 A merging algorithm

In this section, we proposed a merging algorithm for the two dimensional case, which ensures success of the merging process under suitable assumptions.

Before discussing the merging algorithm, it is important to reiterate that  $\Gamma$  is  $C^2$ -smooth and non-self-intersecting, similar to the conditions stated in [26]. For any  $P \in \Gamma$ , denote by  $\kappa(P)$  the curvature of  $\Gamma$  at  $P$ . For any two points  $P_1, P_2 \in \Gamma$ , denote by  $\theta(P_1, P_2)$  the angle between the two tangent lines at  $P_1$  and  $P_2$ . For simplicity, we assume that the mesh  $\mathcal{T}_h$  (before merging) is a Cartesian mesh consisting of squares of the same size  $h$ . Moreover, three additional assumptions are made regarding the mesh  $\mathcal{T}_h$ :

- (I) Among the four edges of any element  $K \in \mathcal{T}_h$ , it is ensured that at most one edge intersects the interface  $\Gamma$  twice (including the endpoints), while the remaining edges intersect the interface at most twice in total.

(II) For any  $P \in \Gamma$ , the ball  $B(P, 2\sqrt{2}h)$  with center  $P$  and radius  $2\sqrt{2}h$  is connected within  $\Omega_i$ ,  $i = 1, 2$ .

(III) For any  $\delta \in (1, \frac{1}{2})$ , which is used in (2.3) to define “small” elements,

$$c_h := h \max_{\substack{P_1, P_2 \in \Gamma \\ |x_1^{P_1} - x_1^{P_2}| \leq h \\ \text{or } |x_2^{P_1} - x_2^{P_2}| \leq h}} \kappa(P_2) \cos(\theta(P_1, P_2))^{-3} \leq \frac{3\sqrt{2}}{4}(1 - 2\delta).$$

**Remark 5.1.** (i) *The Assumption (I) on how the mesh elements are cut by the interface is more general than the assumption commonly adopted in the literature [13], which requires that the interface intersects the boundary of any element twice at different sides. In addition to twice, our Assumption (I) allows the interface to intersect the boundary of an element three or four times (see e.g. the 2nd, 3rd, 6th, and 7th subfigures in Fig. 5.2A).*

(ii) *The Assumption (II) is used to guarantee the success of the merging algorithm (see Algorithm 5.1 and Theorem 5.1 below). It is worth noting that our Assumption (II) is somewhat weaker than the 4th condition of Definition 3.1 in [13], used in their merging algorithm, e.g., the scenario depicted in the Fig. 5.1 below is not permitted in [13], but is allowed in this paper.*

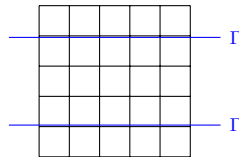


Fig. 5.1

(iii) *Our Assumption (III) says that the change of tangent angles within a step of  $h$  in  $x_1$  and  $x_2$  directions should be appropriately bounded, e.g., less than or equal to  $\frac{\pi}{4}$  if  $\delta = \frac{1}{4}$  and  $\max_{P \in \Gamma} \kappa(P)h \leq \frac{3}{16}$ .*

According to Assumption (I), we have enumerated the allowed interface elements depicted in Fig. 5.2. It is important to note that additional cases can be derived through rotation and symmetry transformations. Therefore, our subsequent analysis will primarily concentrate on the situations depicted in Fig. 5.2. We have categorized these situations into two distinct groups. Within these groups, the merging selection for type-1 elements is unequivocal, as indicated by the dotted square in Fig. 5.2A. However, for type-2 elements, there are two potential merging selections, as illustrated by the dotted squares in Fig. 5.2B, this requires the incorporation of supplementary criteria to discern the merging object, such as the assessment of the intersecting areas within  $\Omega_i$ .

Prior to presenting the algorithm and demonstrating its feasibility, we undertake some preparatory tasks. The following lemma gives a representation of the distance between a  $C^2$  curve and one of its secant lines.

**Lemma 5.1.** *Let  $C$  be a regular  $C^2$  curve and  $A, B$  be two points on  $C$  (see Fig. 5.3). Suppose that any two tangent lines to the curve are not perpendicular to each other. For any point  $P \in C$ , denote by  $P_\perp$  the foot of the perpendicular from  $P$  to the secant line  $\overline{AB}$ . Then there exist a point*

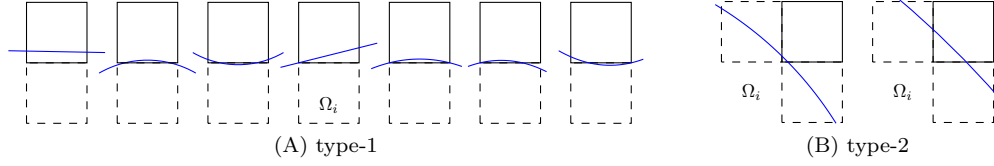


Fig. 5.2: two type small elements

$P_0 \in \mathcal{C}$  between  $A$  and  $B$  and a point  $P_1 \in \mathcal{C}$  between  $P$  and  $A$  or  $B$  such that the distance from  $P$  to the secant line  $\overline{AB}$  is expressed as

$$(5.1) \quad |PP_\perp| = \frac{1}{2} \kappa(P_1) \cos(\theta(P_0, P_1))^{-3} |P_\perp A| |P_\perp B|,$$

where  $\kappa(P_1)$  denotes the curvature of  $\mathcal{C}$  at  $P_1$  and  $\theta(P_0, P_1)$  denotes the angle between the tangent lines to  $\mathcal{C}$  at  $P_0$  and  $P_1$ .

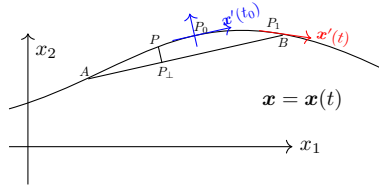


Fig. 5.3: local coordinate system

*Proof.* Let  $\mathbf{x} = \mathbf{x}(t)$  be a parametric representation the curve  $\mathcal{C}$ . Clearly, there exists a point  $P_0 = \mathbf{x}(t_0)$  between  $A$  and  $B$  such that the tangent line at  $P_0$  to  $\mathcal{C}$  is parallel to  $\overline{AB}$ . To proceed, we establish a local coordinate system at the point  $P_0$  with its tangent and normal directions:  $\tilde{\mathbf{x}} = M(\mathbf{x} - \mathbf{x}(t_0))$ , where the rotation matrix,

$$M = \frac{1}{|\mathbf{x}'(t_0)|} \begin{pmatrix} x'_1(t_0) & x'_2(t_0) \\ -x'_2(t_0) & x'_1(t_0) \end{pmatrix} := \begin{pmatrix} m_1 & m_2 \\ -m_2 & m_1 \end{pmatrix}.$$

Since  $\tilde{x}'_1(t) = |\mathbf{x}'(t_0)|^{-1} (x'_1(t_0)x'_1(t) + x'_2(t_0)x'_2(t)) \neq 0$ , the global inverse function theorem [38] implies that the curve can be explicitly expressed as  $\tilde{x}_2 = f(\tilde{x}_1)$ . Then we have  $f'(\tilde{x}_1) = \frac{d\tilde{x}_2}{d\tilde{x}_1} = \frac{-m_2x'_1 + m_1x'_2}{m_1x'_1 + m_2x'_2}$ , and the curvature  $\kappa = \frac{x'_1x''_2 - x'_2x''_1}{|\mathbf{x}'|^3}$ , thus,

$$(5.2) \quad \begin{aligned} f''(\tilde{x}_1) &= \frac{d(f'(\tilde{x}_1))}{d\tilde{x}_1} = \frac{(m_1^2 + m_2^2)(x'_1x''_2 - x'_2x''_1)}{(m_1x'_1 + m_2x'_2)^3} = \kappa(\mathbf{x}(t)) \left( \frac{|\mathbf{x}'(t_0)||\mathbf{x}'(t)|}{\mathbf{x}'(t_0) \cdot \mathbf{x}'(t)} \right)^3 \\ &= \kappa(\mathbf{x}(t)) \cos(\theta(P_0, \mathbf{x}(t)))^{-3}. \end{aligned}$$

Noting that the line  $\overline{AB}$  can be view as the linear Lagrange interpolation of the curve, we have from the interpolation error result that

$$|PP_\perp| = \frac{1}{2} f''(P_1) |P_\perp A| |P_\perp B| = \frac{1}{2} \kappa(P_1) \cos(\theta(P_0, P_1))^{-3} |P_\perp A| |P_\perp B|,$$

where  $P_1 \in \mathcal{C}$  is a point between  $P$  and  $A$  or  $B$ . This completes the proof of the lemma.  $\square$

**Remark 5.2.** *The lemma still holds in the limiting case of  $B \rightarrow A$ , but with the secant line  $\overline{AB}$  replaced by the tangent line at  $A$ ,  $P_0 = A$ , and  $|P_\perp A|$ ,  $|P_\perp B|$  replaced by  $|P_\perp P_0|$ , i.e.,*

$$(5.3) \quad |PP_\perp| = \frac{1}{2} \kappa(P_1) \cos(\theta(P_0, P_1))^{-3} |P_\perp P_0|^2,$$

for some point  $P_1 \in \mathcal{C}$  between  $P$  and  $A$ .

It's worth noting that the formulas (5.1) and (5.3) are independent of the selection of parametric representation of the curve.

The next lemma clarify that, under certain conditions for  $h$ , any ‘‘small’’ elements in  $\mathcal{T}_h$  has a proper ‘‘large’’ neighbouring element.

**Lemma 5.2.** *Suppose that the mesh  $\mathcal{T}_h$  satisfies Assumptions (I)–(III).*

- (i) *For any  $K \in \mathcal{T}_{h,i}^{small}$ , there exists an element  $K' \in \mathcal{T}_{h,i}^{large}$  that can be merged with  $K$ , which means that  $K$  and  $K'$  have a common edge.*
- (ii) *For any  $K' \in \mathcal{T}_{h,i}^{large}$ , there are at most two small elements in  $\mathcal{T}_{h,i}^{small}$  that can be merged with  $K'$ .*

*Proof.* Let us begin by considering  $K$  as a type-1 small element with three typical cases as shown in Fig. 5.4A. In the case depicted on the left side of Fig. 5.4A, it is evident that  $K'$  is entirely contained within  $\Omega_i$  thanks to Assumption (II). Moving to the middle section of Fig. 5.4A, we observe that points  $A$  and  $B$  represent the two intersection points between the boundary of  $K$  and  $\Gamma$ . To facilitate our analysis, we will refer to the shaded area as  $\tilde{K}$ , then from Lemma 5.1 we can get

$$\begin{aligned} |\tilde{K}| &= \int_A^B |PP_\perp| dl = \int_A^B \frac{1}{2} \kappa(P_1) \cos(\theta(P_0, P_1))^{-3} |P_\perp A| |P_\perp B| dl \\ &\leq \frac{1}{2} \frac{c_h}{h} \int_A^B |P_\perp A| |P_\perp B| dl = \frac{1}{12} \frac{c_h}{h} |AB|^3 \leq \frac{c_h}{12} h^2 = \frac{c_h}{12} |K'|. \end{aligned}$$

Here  $\int_A^B \cdot dl$  denotes a integral on the line segment  $\overline{AB}$ . Therefore,  $|K' \cap \Omega_i| \geq (1 - \frac{c_h}{12}) |K'|$ . Similarly, in the right of Fig. 5.4A,

$$|\tilde{K}| = \int_A^B |PP_\perp| dl = \int_A^B \frac{1}{2} \kappa(P_1) \cos(\theta(P_0, P_1))^{-3} |P_\perp P_0|^2 dl \leq \frac{c_h}{6} |K'|,$$

here  $|PP_\perp|$  satisfies equation (5.3), then  $|K' \cap \Omega_i| \geq (1 - \frac{c_h}{6}) |K'|$ . Therefore, for a type-1 small element,  $K'$  is large, since  $1 - \frac{c_h}{6} \geq \delta$  thanks to Assumption (III).

Secondly, if  $K$  is a type-2 small element and  $K'$  is a type-2 interface element as in the left of Fig. 5.4B, the shaded part satisfies that

$$|\tilde{K}| = \int_A^B |PP_\perp| dl = \int_A^B \frac{1}{2} \kappa(P_1) \cos(\theta(P_0, P_1))^{-3} |P_\perp A| |P_\perp B| dl \leq \frac{1}{12} \frac{c_h}{h} |AB|^3 \leq \frac{\sqrt{2}}{6} c_h |K'|,$$

and hence, by Assumption (III),  $|K' \cap \Omega_i| \geq (\frac{1}{2} - \frac{\sqrt{2}}{6} c_h) |K'|$ . On the other hand, if  $K'$  is a type-1 interface element, as depicted on the right side of Fig. 5.4B, we have points  $A$  and  $B$  representing

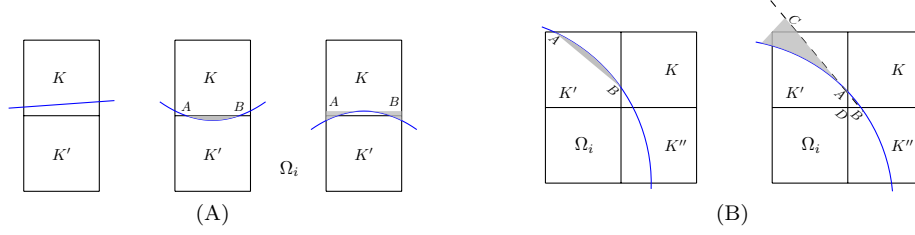


Fig. 5.4

the intersection points between the boundary of  $K$  and  $\Gamma$ , while the vertex  $D$  lies within  $\Omega_i$ . Let us introduce point  $C$  as the projection of the vertex of  $K'$  that is not adjacent to  $D$  onto the line  $AB$ . Now, let us denote the lengths of segments  $AD$  and  $BD$  as  $a$  and  $b$ , respectively. Without loss of generality, let us assume that  $a \geq b$ . Consequently, we can express the length of segment  $AC$  as  $\frac{bh+a(h-a)}{(a^2+b^2)^{1/2}}$ , then we have

$$\begin{aligned}
|\tilde{K}| &= \int_C^A |PP_\perp| dl = \int_C^A \frac{1}{2} \kappa(P_1) \cos(\theta(P_0, P_1))^{-3} |P_\perp A| |P_\perp B| dl \\
&\leq \frac{c_h}{2h} \left( \frac{1}{3} |AC|^3 + \frac{1}{2} |AB| |AC|^2 \right) = \frac{c_h}{h} \frac{2bh + 2ah + a^2 + 3b^3}{12(a^2 + b^2)^{\frac{1}{2}}} \frac{(bh + a(h-a))^2}{a^2 + b^2} \\
&\leq \frac{c_h}{h} \frac{2\sqrt{2}h(a^2 + b^2)^{\frac{1}{2}} + 2a^2 + 2b^2}{12(a^2 + b^2)^{\frac{1}{2}}} (h^2 + (h-a)^2) \leq \frac{c_h}{6h} (\sqrt{2}h + (a^2 + b^2)^{\frac{1}{2}}) (h^2 + (h-a)^2) \\
&\leq \frac{\sqrt{2}c_h}{6h} (h+a)(h^2 + (h-a)^2),
\end{aligned}$$

then

$$|K' \setminus \Omega_i| \leq \frac{1}{2} \frac{b}{a} (h-a)^2 + |\tilde{K}| \leq \frac{1}{2} (h-a)^2 + \frac{\sqrt{2}c_h}{6h} (h+a)(h^2 + (h-a)^2) := g(a).$$

Under Assumption (III), it is easy to find that  $\max_{a \in [0, h]} g(a) = \max \{g(0), g(h)\} = g(0) = \frac{1}{2}h^2 + \frac{\sqrt{2}}{3}c_h h^2$ . Therefore, by Assumption (III),

$$(5.4) \quad |K' \cap \Omega_i| \geq \left( \frac{1}{2} - \frac{\sqrt{2}}{3}c_h \right) |K'| \geq \delta |K'|.$$

This completes the proof of (i).

Next, we prove (ii). Fig. 5.5A illustrates the scenarios of merging two small elements and  $K'$ . It is sufficient to consider the case of three small elements. Let us assume that there are three small elements  $K_1$ ,  $K_2$  and  $K_3$ , which surround and merge with the large element  $K'$ , as depicted in Fig. 5.5B. It is obvious that  $K_4$  and  $K_5$  are not intersected with  $\Gamma$ , as otherwise, according to (i), there would be a large element among  $K_1$ ,  $K_2$  and  $K_3$ . Thus  $K_1$  must be the type-1 element as shown in Fig. 5.5B. We denote the intersections of the boundary of  $K_1$  with  $\Gamma$  by points  $A$  and  $C$ , the intersections of the boundary of  $K_2$  with  $\Gamma$  by points  $B$  and  $E$ , and the two endpoints of the intersecting edge of  $K'$  and  $K_2$  by points  $D$  and  $F$ . It is worth noting that it is simpler when  $E$

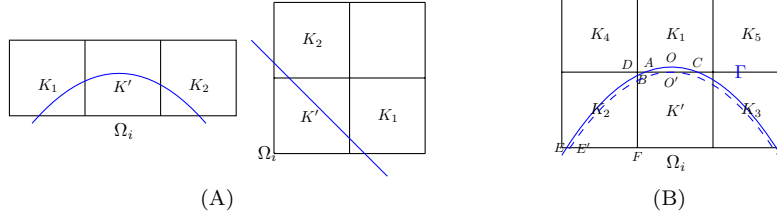


Fig. 5.5

lays on the left edge of  $K_2$ , thus we just discuss the case as shown in Fig. 5.5B. Then let  $O$  be the point whose tangent is parallel to  $AC$ , without loss of generality, we assume that  $O$  is closer to the left boundary of  $K'$ . Then thanks to (5.3), we have  $|BF| = h - |BD| \geq (1 - \frac{ch}{8})h$ . As shown in the Fig. 5.5B, the blue dotted line represents the case when  $\Gamma$  translates downward until point  $O'$  lays on  $AC$ , and  $E'$  is the intersection after translation. Similarly,  $h \leq \frac{ch}{2h}(|E'F| + |O'D|)^2$ , thus  $|EF| \geq |E'F| \geq \frac{\sqrt{2}h}{\sqrt{ch}} - \frac{1}{2}h$ . In the same way with (i), we have

$$|K_2 \cap \Omega_i| \geq \frac{1}{2}|EF||BF| - \frac{1}{12} \frac{ch}{h} (|EF|^2 + |BF|^2)^{\frac{3}{2}}.$$

We can readily demonstrate that the inequality  $|K_2 \cap \Omega_i| \geq \delta|K_2|$  holds through a straightforward calculation. This completes the proof of the lemma.  $\square$

**Remark 5.3.** *In situations where a small element has two potential merging options and chooses at random, both situations in Fig. 5.5A are likely to occur, it is worth noting that our algorithm works for both cases. However, in practical applications, we will choose the best merging, for example, select the element with a larger intersection area with  $\Omega_i$  to merge, then the first situation in Fig. 5.5A probably will not happen.*

Next, we present the merging algorithm, which starts from the pairwise merging according to Lemma 5.2, and ends at dealing with the situation where large elements are merged multiple times. This process completes the definition of macro-element  $M_i(K)$ .

---

**Algorithm 5.1** Merging algorithm

---

**Require:** Mesh satisfying Assumptions (I)–(III).

- 1: **for**  $i = 1, 2$  **do**
- 2:   Let  $N_i(K') = \emptyset, \forall K' \in \mathcal{T}_{h,i}^{large}$ .
- 3:   **for**  $K \in \mathcal{T}_{h,i}^{small}$  **do**
- 4:     Find a neighbor  $K' \in \mathcal{T}_{h,i}^{large}$  for  $K$  according to Lemma 5.2, let  $N_i(K') = N_i(K') \cup \{K\}$ .
- 5:   **end for**
- 6:   **for**  $K' \in \mathcal{T}_{h,i}^{large}, \text{card}(N_i(K')) > 0$  **do**
- 7:     **if**  $\text{card}(N_i(K')) = 1$  **then**
- 8:       Define  $M_i(N_i(K')) = M_i(K') = K' \cup N_i(K')$ .
- 9:     **else**



10:        Let  $\tilde{K}$  be the minimum rectangle containing all elements in  $N_i(K')$  and  $K'$ , define  
               $M_i(K) = \tilde{K}$ , for any  $K \in \mathcal{T}_{h,i}$  contained in  $\tilde{K}$ .  
 11:        **end if**  
 12:        **end for**  
 13:        **end for**

---

The following theorem says that the mesh obtained by the merging algorithm is well-defined.

**Theorem 5.1.** *Suppose that the mesh  $\mathcal{T}_h$  satisfies Assumptions (I)–(III). Let  $\mathcal{M}_h$  be the mesh obtained by the merging Algorithm 5.1. We have for  $i = 1, 2$ , (i)  $\text{diam } K \lesssim h$ , for any  $K \in \mathcal{M}_{h,i}$ , (ii)  $K_1^\circ \cap K_2^\circ = \emptyset$ , for any  $K_1, K_2 \in \mathcal{M}_{h,i}$ .*

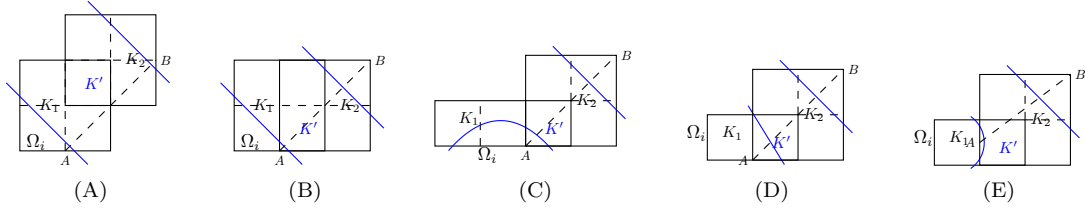


Fig. 5.6: overlap cases

*Proof.* From Lemma 5.2(ii), we have  $\text{card}(N_i(K')) \leq 2$ ,  $\forall K' \in \mathcal{T}_{h,i}^{large}$ , which implies that (i) holds. Next, let's prove (ii). If there exist two macro-elements, denoted as  $K_1$  and  $K_2$ , in  $\mathcal{M}_{h,i}$  such that  $K_1^\circ \cap K_2^\circ \neq \emptyset$ , the second case in Fig. 5.5A must be involved and we designate it as  $K_2$ . Under the constraint imposed by Assumption (I), the situations must align closely with those depicted in Fig. 5.6. Specifically, in Fig. 5.6A, since both points  $A$  and  $B$  belong to  $\Omega_i$  and the distance  $|AB| = 2\sqrt{2}h$ , it implies the existence of a point  $\mathbf{x}_0$  on  $\Gamma$  such that  $B(\mathbf{x}_0, 2\sqrt{2}h) \cap \Omega_i$  is not connected. However, this contradicts Assumption (II). The cases in Fig. 5.6B-5.6E are similar.  $\square$

**Remark 5.4.** (i) *In comparison to the algorithm presented in [13], our algorithm exhibits several notable differences. Firstly, we allow for more kinds of interface elements (see e.g. the 2nd, 3rd, 6th, and 7th subfigures in Fig. 5.2A). Secondly, if we replace the Assumption (II) with the 4th condition of Definition 3.1 in [13], our proof also holds. More prominently, our method, based on the area criterion (2.2) for evaluating elements, imposes the limitation (III) on two geometric variables of the interface together with the mesh size to ensure that the merging process can proceed. This differs from the approach in [13], which introduces the concept of the chain of interface elements to ensure that the algorithm is feasible basing on using the side length criteria to evaluate elements. Furthermore, in this paper, the merging is performed separately for two subregions, which to some extent reduces the complexity of the algorithm.*

(ii) *In practical applications, the merging process is achieved by employing a matrix congruence transformation on the stiffness matrix. Recalling the definitions of the nodal points of the merged DG-FEM spaces  $V_{h,1}$  and  $V_{h,2}$ ,  $\mathcal{N}_{h,1}$  and  $\mathcal{N}_{h,2} \setminus \partial\Omega$  as outlined in (4.1), correspondingly, we denote  $\tilde{\mathcal{N}}_{h,1} = \{\tilde{z}_1^1, \tilde{z}_1^2, \dots, \tilde{z}_1^{\tilde{N}_1}\}$  and  $\tilde{\mathcal{N}}_{h,2} \setminus \partial\Omega = \{\tilde{z}_2^1, \tilde{z}_2^2, \dots, \tilde{z}_2^{\tilde{N}_2}\}$  the sets of nodal points of the DG-FEM spaces before merging, which have the same discontinuity as  $V_{h,1}$  and  $V_{h,2}$  respectively. For any  $v_h \in V_h$ , let  $\tilde{\mathbf{v}} = (v_h(\tilde{z}_1^1), v_h(\tilde{z}_1^2), \dots, v_h(\tilde{z}_1^{\tilde{N}_1}), v_h(\tilde{z}_2^1), v_h(\tilde{z}_2^2), \dots, v_h(\tilde{z}_2^{\tilde{N}_2}))$ . In fact, the merging*

is to treat the vector  $\tilde{\mathbf{v}}$  as an interpolation of  $\mathbf{v}$ , which is defined in (4.1), and the interpolation coefficients are all  $O(1)$ . That is, it is easy to find a matrix  $B$  such that  $\tilde{\mathbf{v}} = B\mathbf{v}$ . Let  $\tilde{A}$  be the stiffness matrix and  $\tilde{F}$  be the right vector without merging, then the stiffness matrix and the right vector for the merged system is given by  $A = B^T \tilde{A} B$  and  $F = B^T \tilde{F}$ .

## 6 Numerical tests

In this section, we illustrate the convergence rates of the proposed methods by some numerical tests. The algorithms are implemented in MATLAB.

The matrix  $\tilde{A}$  and the vector  $\tilde{F}$  may be assembled by using the standard finite element nodal basis functions or their restrictions on either parts of the interface elements in  $\mathcal{T}_\Gamma$  (cf. [39]). Another thing is about calculations of the following two types of integrals on curved surfaces  $K \cap \Gamma$  and curved subdomains  $K_i = K \cap \Omega_i$ ,  $i = 1, 2$  for  $K \in \mathcal{T}_\Gamma$ , which are involved in assembling  $\tilde{A}$  and  $\tilde{F}$ .

$$(6.1) \quad Q_1 = \int_{K \cap \Omega_i} F(x, y) d\sigma \quad \text{and} \quad Q_2 = \int_{K \cap \Gamma} F(x, y) ds.$$

As in [26], we transform the integral domain to a proper reference domain and then resort to the one dimensional Gauss quadrature rules. We omitted the details. The influence of quadrature formulas as well as the approximation of the interface on the error estimates will be considered in a separate work. We refer to [10, 28, 29] for analyses of geometry error for some unfitted finite element methods and refer to [17, 22, 28, 34, 36] for works on computing integrals on the domain with curved boundary.

**Example 6.1.** *The domain  $\Omega$  is the unit square  $(0, 1) \times (0, 1)$  and the interface  $\Gamma$  is a 5 petal flower with center  $(0.5, 0.5)$ , which is characterized as follows:*

$$R = \frac{1}{2} + \frac{1}{7} \sin 5\theta,$$

where  $(R, \theta)$  are the polar coordinates of the pole at  $(\frac{1}{2}, \frac{1}{2})$ . We will use the Cartesian meshes to partition the domain  $\Omega$  into squares of the same size  $h$  (see e.g. Fig. 2.1).  $f$ ,  $g_D$  and  $g_N$  are so chosen that the exact solution to the interface problem (2.1) is the following piecewise smooth function (see Fig. 6.1):

$$(6.2) \quad u(x, y) = \begin{cases} \frac{1}{\alpha_1} \exp(xy), & (x, y) \in \Omega_1, \\ \frac{1}{\alpha_2} \sin(\pi x) \sin(\pi y), & (x, y) \in \Omega_2, \end{cases}$$

where

$$\alpha_1 = 1, \alpha_2 = 1000 \quad \text{or} \quad \alpha_1 = 1000, \alpha_2 = 1.$$

Next we show results for the SUIPDG-FEM. We set the penalty parameter to be  $\gamma = 100$  as in [26]. We first examine the  $h$ -convergence rate of the SUIPDG-FEM. Denote the energy norm by

$$|v|_{1,h} := \|\alpha^{\frac{1}{2}} \nabla v\|_{0, \Omega_1 \cup \Omega_2}.$$

Fig. 6.2 shows the results on the relative energy norm errors for both choices of the coefficient  $\alpha(x)$  and  $p = 1, 2, 3$ . The convergence rate of  $O(h^p)$  is observed in all cases, which verify the theoretical

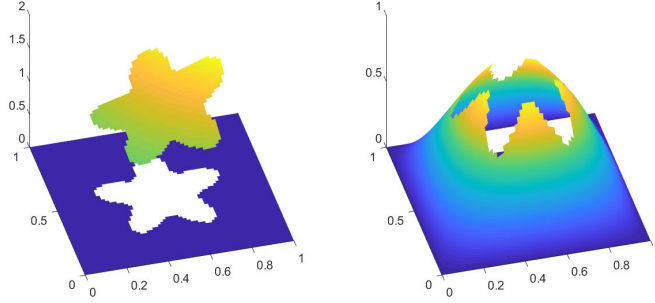


Fig. 6.1: Surface plots of  $u(x)$ . Left:  $\alpha_1 = 1, \alpha_2 = 1000$ . Right:  $\alpha_1 = 1000, \alpha_2 = 1$ .

estimate (3.18). And Fig. 6.3 shows the results on the relative  $L^2$  errors. They all match the convergence order proved in Theorem 3.2, which is  $O(h^{p+1})$ , except the last few steps in Fig. 6.3 when  $p = 3$ . The authors think it should be caused by the round off errors, after all, the relative error in the  $L^2$ -norm has been less than  $10^{-10}$  for the last few steps when  $p = 3$ . Then we examine the  $h$ -convergence rate of flux error. Fig. 6.4 shows that convergence rate for the relative flux error of  $O(h^p)$  is observed in all cases, which verify the theoretical estimate in Theorem 3.3.

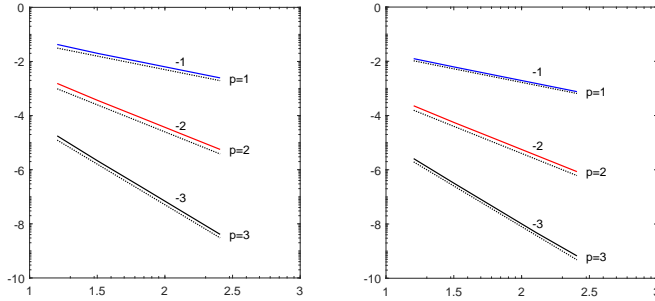


Fig. 6.2:  $\ln \frac{|u-u_h|_{1,h}}{|u|_{1,h}}$  versus  $\ln \frac{1}{h}$  with  $h = \frac{1}{20}, \frac{1}{32}, \dots, \frac{1}{256}$  for  $p = 1, 2, 3$ , respectively. Left:  $\alpha_1 = 1, \alpha_2 = 1000$ . Right:  $\alpha_1 = 1000, \alpha_2 = 1$ . The dotted lines give reference lines of slopes  $-1, -2$ , and  $-3$ , respectively.

For readers who may be interested, we also provide numerical results on the relative errors in some discrete  $L^\infty$ -norm  $\|\cdot\|_{\infty,h}$  in Fig. 6.5, although the theoretical analysis has not been done in this work. Here the discrete  $L^\infty$ -norm  $\|\cdot\|_{\infty,h}$  is defined as the maximum of the errors at the nodal points contained in  $\bar{\Omega}_1$  and  $\bar{\Omega}_2$ , respectively. The convergence rate of  $O(h^{p+1})$  is observed in all cases before the round of errors take effect.

Next we examine the condition number of the stiffness matrix of SUIPDG-FEM. Fig. 6.6 shows that  $\kappa(A) = O(h^{-2})$  which verifies the estimate in Theorem 4.1 since  $\frac{\alpha_{max}}{\alpha_{min}} = 1000$  is fixed.

Finally, we examine the influence of the jump of the coefficient. We fix the mesh size  $h = \frac{1}{32}$ .

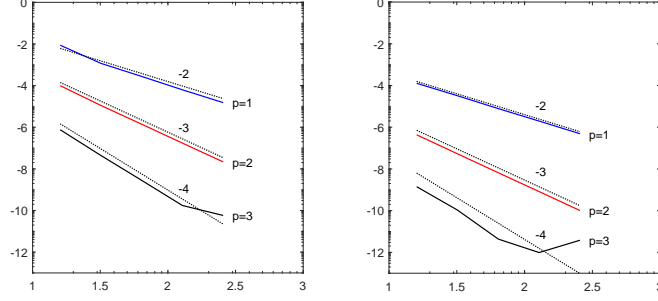


Fig. 6.3:  $\ln \frac{\|u - u_h\|_{0,\Omega}}{\|u\|_{0,\Omega}}$  versus  $\ln \frac{1}{h}$  with  $h = \frac{1}{20}, \frac{1}{32}, \dots, \frac{1}{256}$  for  $p = 1, 2, 3$ , respectively. Left:  $\alpha_1 = 1, \alpha_2 = 1000$ . Right:  $\alpha_1 = 1000, \alpha_2 = 1$ . The dotted lines give reference lines of slopes  $-2, -3$ , and  $-4$ , respectively.

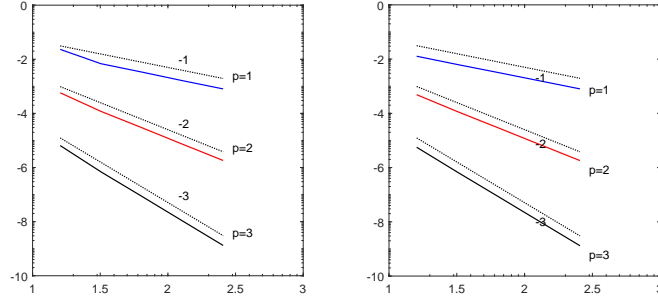


Fig. 6.4:  $\ln \frac{\|\alpha \nabla(u - u_h)\|_{0,\Omega}}{\|\alpha \nabla u\|_{0,\Omega}}$  versus  $\ln \frac{1}{h}$  with  $h = \frac{1}{20}, \frac{1}{32}, \dots, \frac{1}{256}$  for  $p = 1, 2, 3$ , respectively. Left:  $\alpha_1 = 1, \alpha_2 = 1000$ . Right:  $\alpha_1 = 1000, \alpha_2 = 1$ . The dotted lines give reference lines of slopes  $-1, -2$ , and  $-3$ , respectively.

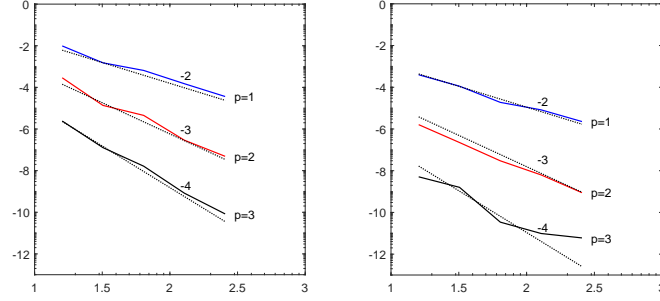


Fig. 6.5:  $\ln \frac{\|u-u_h\|_{\infty,h}}{\|u\|_{\infty,h}}$  versus  $\ln \frac{1}{h}$  with  $h = \frac{1}{20}, \frac{1}{32}, \dots, \frac{1}{256}$  for  $p = 1, 2, 3$ , respectively. Left:  $\alpha_1 = 1, \alpha_2 = 1000$ . Right:  $\alpha_1 = 1000, \alpha_2 = 1$ . The dotted lines give reference lines of slopes  $-2, -3$ , and  $-4$ , respectively.

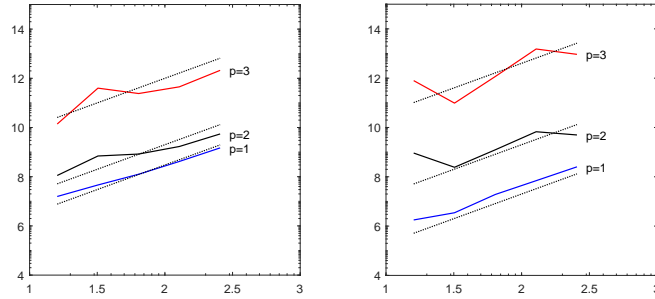


Fig. 6.6:  $\ln \kappa(A)$  versus  $\ln \frac{1}{h}$  with  $h = \frac{1}{20}, \frac{1}{32}, \dots, \frac{1}{256}$  for  $p = 1, 2, 3$ , respectively. Left:  $\alpha_1 = 1, \alpha_2 = 1000$ . Right:  $\alpha_1 = 1000, \alpha_2 = 1$ . The dotted lines give reference lines of slope 2.

Fig. 6.7 (a)-(c) plots  $\ln \frac{|u-u_h|_{1,h}}{|u|_{1,h}}$ ,  $\ln \frac{\|u-u_h\|_{0,\Omega}}{\|u\|_{0,\Omega}}$ , and  $\ln \frac{\|u-u_h\|_{\infty,\Omega}}{\|u\|_{\infty,\Omega}}$ , versus  $\ln(\alpha_2/\alpha_1)$  respectively. It indicates that the relative  $H^1$ ,  $L^2$ , and  $L^\infty$  errors convergence as  $\frac{\alpha_{max}}{\alpha_{min}} \rightarrow \infty$ , which means that they are all independent of the jump of the coefficient. Fig. 6.7 (d) plots  $\ln(\kappa(A))$ , versus  $\ln(\alpha_2/\alpha_1)$  which shows that the condition number  $\kappa(A)$  depends on  $\frac{\alpha_{max}}{\alpha_{min}}$  linearly and hence verifies (4.11).

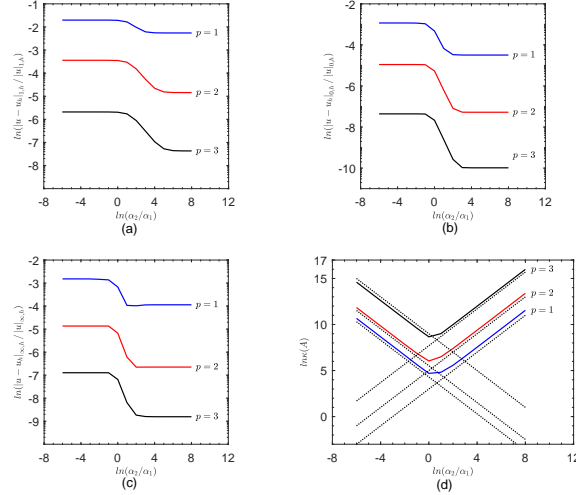


Fig. 6.7: Ln-ln plots of the relative errors in  $H^1$ -,  $L^2$ -,  $L^\infty$ -norms ((a), (b), (c)), and  $\kappa(A)$  ((d)) versus  $\alpha_2/\alpha_1$  with  $(\alpha_1, \alpha_2) = (10^6, 1), (10^5, 1), \dots, (1, 1), (1, 10), \dots, (1, 10^8)$ , for  $p = 1, 2, 3$ , respectively. The dotted lines in (d) give reference lines of slopes -1 or 1.

**Example 6.2.** The computational domain is  $(0, 1) \times (0, 1)$ , and the interface  $\Gamma$  is the circle given by  $(x - \frac{1}{2})^2 + (y - \frac{1}{2})^2 = \frac{1}{8}$ . The exact solution  $u$  is chosen as

$$(6.3) \quad u(x, y) = \begin{cases} \frac{1}{\alpha_1} (\frac{1}{8} - ((x - \frac{1}{2})^2 + (y - \frac{1}{2})^2)) \sin(\pi x) \sin(\pi y), & (x, y) \in \Omega_1, \\ \frac{1}{\alpha_2} (\frac{1}{8} - ((x - \frac{1}{2})^2 + (y - \frac{1}{2})^2)) \sin(\pi x) \sin(\pi y), & (x, y) \in \Omega_2, \end{cases}$$

which has vanishing jumps at the interface both in the solution and the flux, and define the source function  $f$  to match the solution.

Fig. 6.8 shows the optimal convergence behavior of one relative error for flux  $\frac{\|\alpha \nabla(u-u_h)\|_{0,h}}{\|f\|_{p-1,h}}$ , and confirms the theoretical prediction deduced by (3.27) and (3.24), the relative error for flux is independent of the jump of the coefficient as well as the relative position of the interface to the mesh.

Since the numerical results for the NUIPDG-FEM with  $\beta = -1$  and the penalty-free NUIPDG-FEM with  $\gamma = 0$  are much similar as those for the SUIPDG-FEM, we omitted them to save space. While the penalty-free NUIPDG-FEM exhibits non-symmetry, it performs with comparable efficiency to the SUIPDG-FEM in nearly all cases, and often with greater simplicity. The rigorous analysis of penalty-free NUIPDG-FEM will be done in a further work.

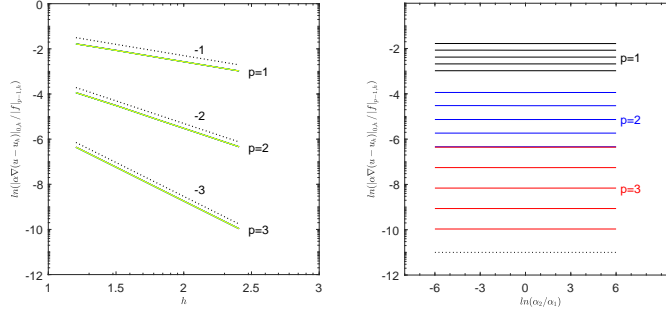


Fig. 6.8: The left is a ln-ln plot of the relative errors in flux versus  $\frac{1}{h}$  with  $h = \frac{1}{16}, \frac{1}{32}, \dots, \frac{1}{256}$ , for  $p = 1, 2, 3$  and  $(\alpha_1, \alpha_2) = (10^6, 1), (10^3, 1), (1, 1), (1, 10^3), (1, 10^6)$ , respectively; and the right is versus  $\alpha_2/\alpha_1$  with  $(\alpha_1, \alpha_2) = (10^6, 1), (10^3, 1), (1, 1), (1, 10^3), (1, 10^6)$ , for  $p = 1, 2, 3$  and  $h = \frac{1}{16}, \frac{1}{32}, \dots, \frac{1}{256}$ , respectively. The dotted lines give reference lines.

## References

- [1] D. Arnold. An interior penalty finite element method with discontinuous elements. *SIAM J. Numer. Anal.*, 19:742–760, 1982.
- [2] I. Babuška. The finite element method with Lagrangian multipliers. *Numer. Math.*, 20:179–192, 1972/73.
- [3] S. Badia, F. Verdugo, and A. F. Martín. The aggregated unfitted finite element method for elliptic problems. *Comput. Methods Appl. Mech. Engrg.*, 336:533–553, 2018.
- [4] P. Bastian and C. Engwer. An unfitted finite element method using discontinuous Galerkin. *Int. J. Numer. Meth. Engrng*, 79(12):1557–1576, 2009.
- [5] E. Burman. Ghost penalty. *Comptes Rendus Mathematique*, 348:1217–1220, 2010.
- [6] E. Burman, M. Cicuttin, G. Delay, and A. Ern. An unfitted hybrid high-order method with cell agglomeration for elliptic interface problems. *SIAM J. Sci. Comput.*, 43(2):A859–A882, 2021.
- [7] E. Burman and A. Ern. Continuous interior penalty  $hp$ -finite element methods for advection and advection-diffusion equations. *Math. Comp.*, 259:1119–1140, 2007.
- [8] E. Burman and A. Ern. An unfitted hybrid high-order method for elliptic interface problems. *SIAM Journal on Numerical Analysis*, 56(3):1525–1546, 2018.
- [9] E. Burman, J. Guzmán, M. A. Sánchez, and M. Sarkis. Robust flux error estimation of an unfitted Nitsche method for high-contrast interface problems. *IMA J. Numer. Anal.*, 38(2):646–668, 2018.
- [10] E. Burman, P. Hansbo, and M. G. Larson. A cut finite element method with boundary value correction. *Math. Comp.*, 87(310):633–657, 2018.

- [11] E. Burman and P. Zunino. A domain decomposition method based on weighted interior penalties for advection-diffusion-reaction problems. *SIAM J. Numer. Anal.*, 44(4):1612–1638, 2006.
- [12] Z. Q. Cai, X. Ye, and S. Zhang. Discontinuous Galerkin finite element methods for interface problems: a priori and a posteriori error estimations. *SIAM J. Numer. Anal.*, 49:1761–1787, 2011.
- [13] Z. Chen and Y. Liu. An arbitrarily high order unfitted finite element method for elliptic interface problems with automatic mesh generation. *J. Comput. Phys.*, 491:Paper No. 112384, 24, 2023.
- [14] Z. Chen and J. Zou. Finite element methods and their convergence for elliptic and parabolic interface problems. *Numer. Math.*, 79:175–202, 1998.
- [15] C. Chu, I. G. Graham, and T. Hou. A new multiscale finite element method for high-contrast elliptic interface problems. *Math. Comp.*, 79(272):1915–1955, 2010.
- [16] P. G. Ciarlet. *The Finite Element Method for Elliptic Problems*. North-Holland, Amsterdam, 1978.
- [17] T. Cui, W. Leng, H. Liu, L. Zhang, and W. Zheng. High-order numerical quadratures in a tetrahedron with an implicitly defined curved interface. *ACM Trans. Math. Software*, 46(1):Art. 3, 18, 2020.
- [18] A. Ern and J. Guermond. Evaluation of the condition number in linear systems arising in finite element approximations. *M2AN*, 40:29–48, 2006.
- [19] A. Ern and J.-L. Guermond. *Theory and Practice of Finite Elements*. Springer-Verlag, New York, 2004.
- [20] A. Ern, A. F. Stephansen, and P. Zunino. A discontinuous Galerkin method with weighted averages for advection-diffusion equations with locally small and anisotropic diffusivity. *IMA J. Numer. Anal.*, 29:235–256, 2009.
- [21] X. Feng and H. Wu. Discontinuous Galerkin methods for the Helmholtz equation with large wave numbers. *SIAM J. Numer. Anal.*, 47:2872–2896, 2009.
- [22] T. Fries and S. Omerović. Higher-order accurate integration of implicit geometries. *Int. J. Numer. Meth. Engng*, 106:323–371, 2016.
- [23] V. Girault and P.-A. Raviart. *Finite element methods for Navier-Stokes equations*, volume 5 of *Springer Series in Computational Mathematics*. Springer-Verlag, Berlin, 1986. Theory and algorithms.
- [24] A. Hansbo and P. Hansbo. An unfitted finite element method, based on Nitsche’s method, for elliptic interface problems. *Comput. Methods Appl. Mech. Engrg.*, 191:5537–5552, 2002.
- [25] J. Huang and J. Zou. Uniform a priori estimates for elliptic and static Maxwell interface problems. *Discrete and Continuous Dynamical Systems, Series B*, 7(1):145–170, 2007.
- [26] P. Huang, H. Wu, and Y. Xiao. An unfitted interface penalty finite element method for elliptic interface problems. *Comput. Methods Appl. Mech. Engrg.*, 323:439–460, 2017.



- [27] A. Johansson and M. G. Larson. A high order discontinuous Galerkin Nitsche method for elliptic problems with fictitious boundary. *Numer. Math.*, 123:607–628, 2013.
- [28] C. Lehrenfeld. High order unfitted finite element methods on level set domains using isoparametric mappings. *Comput. Methods Appl. Mech. Engrg.*, 300:716–733, 2016.
- [29] C. Lehrenfeld and A. Reusken. Analysis of a high-order unfitted finite element method for elliptic interface problems. *IMA J. Numer. Anal.*, 38(3):1351–1387, 2018.
- [30] J. Li, J. M. Melenk, B. Wohlmuth, and J. Zou. Optimal a priori estimates for higher order finite elements for elliptic interface problems. *Appl. Numer. Math.*, 60:19–37, 2010.
- [31] R. Li and F. Yang. A discontinuous Galerkin method by patch reconstruction for elliptic interface problem on unfitted mesh. *SIAM J. Sci. Comput.*, 42(2):A1428–A1457, 2020.
- [32] T. Lin, Y. Lin, and X. Zhang. Partially penalized immersed finite element methods for elliptic interface problems. *SIAM J. Numer. Anal.*, 53(2):1121–1144, 2015.
- [33] R. Massjung. An unfitted discontinuous Galerkin method applied to elliptic interface problems. *SIAM J. Numer. Anal.*, 50:3134–3162, 2012.
- [34] B. Müller, F. Kummer, and M. Oberlack. Highly accurate surface and volume integration on implicit domains by means of moment-fitting. *Internat. J. Numer. Methods Engrg.*, 96:512–528, 2013.
- [35] J. A. Nitsche. über ein variationsprinzip zur lösung Dirichlet-Problemen bei Verwendung von Teilräumen, die keinen Randbedingungen unterworfen sind. *Abh. Math. Sem. Univ. Hamburg*, 36:9–15, 1971.
- [36] R. I. Saye. High-order quadrature methods for implicitly defined surfaces and volumes in hyperrectangles. *SIAM J. Sci. Comput.*, 37:A993–A1019, 2015.
- [37] Q. Wang and J. Chen. An Unfitted Discontinuous Galerkin Method for Elliptic Interface Problems. *Journal of Applied Mathematics*, 2014(none):1 – 9, 2014.
- [38] F. Wu and C. Desoer. Global inverse function theorem. *IEEE Transactions on Circuit Theory*, 19(2):199–201, March 1972.
- [39] H. Wu and Y. Xiao. An unfitted hp-interface penalty finite element method for elliptic interface problems. *J. Comput. Math.*, 37:316–339, 2019.
- [40] Y. Xiao, J. Xu, and F. Wang. High-order extended finite element methods for solving interface problems. *Comput. Methods Appl. Mech. Engrg.*, 364:112964, 21, 2020.